Sedimentology, faunal content and pollen record of Middle Pleistocene palustrine and lagoonal sediments from the Peri-Adriatic basin, Abruzzi, eastern central Italy

Pierluigi Pieruccini[a], Claudio Di Celma[b], Federico Di Rita[c], Donatella Magri[c], Giorgio Carnevale[d], Piero Farabollini[b], Luca Ragaini[e], Mauro Caffau[f]

[a]Department of Physical Sciences, Earth and Environment, University of Siena, Siena, Italy
[b]School of Science and Technology, University of Camerino, Camerino, Italy
[c]Department of Environmental Biology, SAPIENZA University of Rome, Rome, Italy
[d]Department of Earth Sciences, University of Turin, Turin, Italy
[d]Department of Earth Sciences, University of Pisa, Pisa, Italy
[f]OGS (National Institute of Oceanography and Experimental Geophysics), Sgonico (TS), Italy

Corresponding author: claudio.dicelma@unicam.it

Abstract

A 25 m-thick outcrop section exposed at Torre Mucchia, on the sea-cliff north of Ortona, eastern central Italy, comprises a rare mid-Pleistocene succession of shallow-water and paralic sediments along the western Adriatic Sea. An integrated study of the section, including facies and microfacies analyses and characterization of paleobiological associations (mollusks, fishes, ostracods, foraminifers and pollen), enable a detailed reconstruction of the paleoenvironmental and paleoclimatic conditions during deposition. The shallow-water deposits include a transgressive, deepening- and fining-upward shoreface to offshore-transition facies succession overlain by a regressive shoreface-foreshore sandstone body with an erosive base and a rooted and pedogenically altered horizon at the top that imply deposition during sea-level fall. This forced regressive unit is overlain by paralic strata forming a transgressive succession comprising palustrine carbonates and back-barrier lagoonal mudstones. The palustrine carbonates exhibit some of the typical features encountered in palustrine limestones deposited within seasonal freshwater wetlands (marl prairies). Following the sea-level rising trend, the freshwater marshes were abruptly replaced by a barrier-lagoon system that allowed deposition of the

overlying mud-rich unit. Within these deposits, the faunal assemblages are consistent with a low-energy brackish environment characterized by a relatively high degree of confinement. The pollen record documents the development of open forest vegetation dominated by *Pinus* and accompanied by a number of mesophilous and thermophilous tree taxa, whose composition supports a tentative correlation with Marine Oxygen Stage 17. The new pollen record from Torre Mucchia improves our understanding of the vegetation development in the Italian Peninsula during the Middle Pleistocene and sheds new light on the role played by the most marked glacial periods in determining the history of tree taxa.

Keywords: Middle Pleistocene, Micropaleontology, Pollen, Mollusks, Fishes, MIS 17, Palustrine carbonates

Introduction

Nearshore, palustrine, and lagoon systems are very sensitive to variations in sea level and/or sediment availability and their sediments represent ideal targets to assess past and present climate changes (e.g. Rossi et al., 2011; Amorosi et al., 2012, 2013; Sarti et al., 2015). The present contribution illustrates and interprets for the first time the paleontological content of nearshore and paralic strata exposed at the top of the middle Pleistocene Qm2 Unit in eastern central Italy. The studied section is the richest source of paralic mollusk, fish, and pollen assemblages documented so far in the Middle Pleistocene of the western Adriatic Sea and provides a rare opportunity to increase the modest knowledge available on these faunas and floras.

A 25 m-thick outcrop section of shallow-water and paralic sediments was studied through a multidisciplinary approach involving a detailed description of sedimentary facies and analysis of micropaleontological (planktonic and benthic foraminifers, ostracods and pollen) and macropaleontological (mollusks and fishes) fossil assemblages. Identification of this fauna and flora has significance for understanding the overall paleoecological settings and climatic conditions in which these sediments were deposited.

Geological setting

The central Apennines are part of an E-NE verging fold-and-thrust belt built up since the Late Oligocene in response to the westward subduction of the Adria micro-plate (i.e., a promontory of the Africa Plate) underneath the European Plate (Malinverno and Ryan, 1986; Ricci Lucchi, 1986; Doglioni, 1991). Progressive tectonic accretion and loading of subducting lithosphere in the Apennine subduction complex (Doglioni, 1991) resulted in the development of a highly articulated foreland basin system at the front of the chain, filled up by relatively thick, diachronous turbidite successions (Ricci Lucchi, 1986). Thrust fronts propagated toward the foreland, involving progressively younger and easternmost foredeep deposits into the orogenic wedge and, at the same time, gradually shifted the depocenters of both foredeep and wedge-top basins further to the east (i.e., Ricci Lucchi, 1986; Ori et al., 1991; Artoni, 2013). The Plio-Pleistocene Peri-Adriatic foredeep records the latest evolutionary stages of the Apennines chain and extends from the Po Plain to the north to the Gulf of Taranto to the south (Fig. 1A). During the latest Miocene to Pleistocene time interval the shape of the central portion of the Peri-Adriatic foredeep, also known as the Pescara depocenter (Ghielmi et al., 2013), was affected by a large variability in space through time, ranging from regular elongated shape to irregular shape, from simple foredeep to fragmented foredeep (Ori et al., 1991). The Quaternary depositional and structural history of this central portion is framed into a large-scale sequence-stratigraphic scheme (Cantalamessa et al., 1986). Specifically, within the traditional subdivision into Quaternary marine (Qm) and Quaternary continental (Qc) unconformity-bounded stratigraphic units, regionally correlatable unconformities divide the Quaternary portion of the basin fill into three major allogroups (Qm1, Qm2, and Qc from oldest to youngest). The unconformities separating these units are well recognizable along the basin margins and document the combined effects of global climate changes and phases of basin reorganization linked to the effects of long-term and regional-scale tectonics (e.g., Ori et al., 1991; Artoni, 2013; Bigi et al., 2013). Overall, these allogroups record a pronounced regressive trend recorded by an upward progression from slope and shelf mudstones of Qm1 (Cantalamessa et al., 2009; Di Celma, 2011; Di Celma et al., 2010, 2013, 2014, 2016a) through littoral sandstones and conglomerates of Qm2 (Cantalamessa and Di Celma, 2004; Di Celma et al., 2016b) to conglomerate-dominated fluvial deposits of Qc (Di Celma et al., 2015). Outcrop equivalents of the Qm and Qc units, displaying strong similarities in terms of both lithology and vertical stacking of facies, have been

identified along the Adriatic side of Italy in the Emilia, Marche, and Molise Apennines (Cantalamessa and Di Celma, 2004; Amorosi et al., 2009; Bracone et al., 2012a, 2012b; Gunderson et al., 2014). By early Calabrian times onwards, the thrust-related structures ceased to be active and the central Peri-Adriatic foredeep was uplifted at an average rate of 0.8–1.0 m/ka (Centamore and Nisio, 2003; Pizzi, 2003).

Study area and methodology

Di Celma et al. (2016a) subdivided the sediments of the Middle Pleistocene Qm2 Unit exposed within the Ortona area, eastern central Italy (Fig. 1), into a stack of three unconformity-bounded sequences, namely $Qm2_3$, $Qm2_2$, and $Qm2_1$ from older to younger. Given that this study examines the distal outcrops of the Qm2 Unit, the top-down nomenclature allows potentially older sequences to be identified and consecutively numbered in the extensive exposures of the Qm2 Unit that continues to the west. The present study documents the stratigraphic context, paleontological content and related paleoenvironmental signal of shallow-water and paralic sediments exposed along coastal cliffs to the north of Ortona, where the upper portion of $Qm2_2$ and the lower portion of the overlying $Qm2_1$ crop out. The studied sedimentary section is difficult to access because the vertical cliffs are more than 20 m high. Only one locality, called Torre Mucchia (42° 22.677'N - 14° 22.595'E) was found safely accessible (Fig. 2A). The section was measured on a decimeter resolution and the sedimentological characterization of the individual facies associations was focused on the registration of lithology, grain size, primary sedimentary structures, degree and type of bioturbation, paleosols, and the presence of fossils and accessory materials, including roots and plant fragments.

Field observations and measurements of the cemented chalky limestones have been integrated with sampling of oriented sediment blocks for micromorphological and microfacies analysis. Eight large hand samples were collected and thin sections were prepared from each of them. Thin sections were examined and described following Stoops (2003), Alonso-Zarza and Wright (2010), Freytet and Verrecchia (2002) and Durand et al. (2010). Large gastropod specimens, preserved as molds, were manually collected directly in the field.

Quantitative analyses on pollen were performed on a total of 29 samples, collected at about 0.2 m intervals along the lower 8 m of the overlying sandy mudstones and prepared according to standard maceration procedures, including treatment with HCl (10%), HF (50%), and NaOH (10%) for 10 minutes. Only 12 samples contained suitable pollen concentrations, in a modest state of preservation. The raw counts of pollen analysis are presented as Supplementary Material. The results of pollen analysis are represented as a percentage diagram plotted by means of the program Psimpoll 4.27 (Bennett, 2009).

Four bulk sediment samples were collected at 2 m intervals for micropalaeontological (ostracods and foraminifers) analyses from the same stratigraphic interval. Approximately 100 g of sediment were picked from each sample, dried at 50°C for 24 h and soaked in water plus H_2O_2 (10%) for 12 h. The samples were subsequently washed under running water through a 63 μm mesh, dried again, and then observed under a binocular microscope.

The primary source of paleontological remains (ostracods, foraminifers, fishes and mollusks) in the studied succession is a 0.4 m thick, mollusk-dominated fossiliferous interval embedded within the lagoon sediments (Fig. 2A, B). Fish otoliths and mollusks were obtained from the processing of a 20 kg bulk sample amalgamated from multiple replicates (5 kg each) collected from different lateral spots of this rich fossiliferous horizon. The shell-rich sediments were disaggregated in a solution of water and H_2O_2 (10%), sieved through 1 mm mesh sieves with tap water and then dried. The residue from the sample was sorted a few grains at a time, and all otoliths and mollusks were handpicked from the remaining sediment. Overall, both fish otoliths and mollusks are relatively well preserved and fine structures necessary for taxonomic identification are usually clearly recognizable.

Results

The Middle Pleistocene Qm2 Unit exposed north of Ortona comprises an interval up to 36 m thick of weakly consolidated sandstones, mudstones, conglomerates and minor carbonates, deposited in a variety of continental, paralic, and shallow-marine environments. The detailed sequence stratigraphic interpretation, based on key surfaces and stratal units that are traceable across the entire study area, has been presented elsewhere (Di Celma et al., 2016a) and is not reiterated here. The description and

interpretation of the five facies associations documented in the studied section are provided below, whereas a view of their vertical stacking pattern is shown in Figure 2C.

Facies associations

In the 25 m-thick studied succession (upper portion of $Qm2_2$ and lower portion of $Qm2_1$), the sedimentological analyses led to distinguish five major facies associations. In ascending order, these facies associations are described below in terms of sedimentological and paleontological features. Figure 2C shows a synthetic interpretation of the outcrop section.

Lower shoreface bioturbated massive sandstone (LSh)

This facies association is 5 m thick and consists of thoroughly bioturbated, fine- to medium-grained silty sandstones. These sediments are generally structureless, although poorly preserved mm-scale plane-parallel and low-angle laminations can locally be identified.

Fragments of marine mollusks and rare well-rounded extraformational clasts averaging 1-1.5 cm in diameter occur randomly scattered throughout the facies association. Discrete intervals of soft sediment-deformed sandstone beds, as much as 1.5 m thick and characterized by recumbent folds, occur intermittently along the outcrop belt, more often at the top of this facies association and close to its vertical transition with the overlying offshore-transition facies association.

The ichnofossil assemblage is largely dominated by unusually large, densely packed, irregularly meandering, horizontal to gently inclined, cylindrical to subcyclindrical, unbranched burrows of *Macaronichnus* sp., but also comprises some isolated burrows of *Rosselia socialis*, a vertically-oriented spindle- to funnel-shaped, mud-lined tube, and *Skolithos linearis*.

The overall paucity of physical sedimentary structures, restricted to the presence of rare plane-parallel and low-angle laminations, the absence of storm-induced sedimentary structures, such as hummocky and swaley cross-stratification, and the pervasively burrowed fabric, indicate that storm waves and currents did not deposit beds significantly thick enough to shield them from total reworking by burrowing organisms and that low-energy conditions prevailed during deposition of this facies association. Unstable sea-floor conditions are indicated by the occurrence of soft-sediment structures.

Triggering mechanisms are unknown, but this instability may have been imparted by seismic disturbances or, less likely, by infrequent large magnitude storms.

The *Macaronichnus* burrows record intrastratal trails produced by infaunal detritus-feeding polychaete worms. With the exception of their unusually large size, the Torre Mucchia *Macaronichnus* burrows are morphologically very similar to those of standard (small) *Macaronichnus segregatis* described by Clifton and Thompson (1978). Similar large *Macaronichnus* burrows have been reported from both ancient (Nara, 2002; Aguirre et al., 2010) and modern (Seike et al., 2011) shoreface deposits. Trace-fossil assemblages overwhelmingly dominated by robust deposit-feeding structures, such as large *Macaronichnus* and *Rosselia*, and with subordinate traces of suspension-feeding organisms, such as *Skolithos*, corresponds to a proximal expression of the *Cruziana* Ichnofacies (Pemberton et al., 2012 and references therein). Both the sedimentary features and the trace fossils of this facies association indicate that deposition occurred above fair-weather wave base, in a well oxygenated, low-energy lower-shoreface setting with infrequent storm influence.

Offshore-transition bioturbated mudstones and fine grained sandstones (OfTr)

At Torre Mucchia this facies association is a 5 m-thick, thoroughly burrowed mixture of sandstone and mudstone. Sandstones are fine-grained and generally preserved in rare, sharp based layers that range from mm- to cm-scale thicknesses and show hints of some horizontal planar to low-angle laminations. Mudstones are characterized by bed-scale variations from moderately to thoroughly bioturbated silty mudstones. Pervasive bioturbation, however, is very common and obscures most of remnant physical sedimentary structures, rendering an overall churned fabric to this facies association. Mollusk shells are present but sparse and consist primarily of disarticulated bivalves found either dispersed throughout this facies or as small clumps. Apart from some little clumps of *Ostrea edulis*, characterizing faunal elements at the outcrop level are the infaunal species *Panopea glycymeris*, mainly preserved as conjoined individuals in vertical (life) or weak oblique position, and *Glycymeris nummaria* (= *violacescens*) preserved both as single and articulated valves. Sparse remains of *Pinna* sp. consist of single, very fragmented valves.

This facies association preserves a record of alternating high- and low-energy conditions. The burrowed mudstones reflect periods of fair-weather conditions and deposition of mud from suspension.

The interbedded sharp-based, horizontal planar to low-angle laminated sandstone beds suggest deposition during episodic storms, when sand was eroded from the upper part of the shoreface and transported basinward. Due to their limited thickness and the intense reworking by burrowing organisms, the preservation potential of these sandstone beds was low.

The macrofossil fauna documented within this facies association is composed of still living species (*P. glycymeris, G. nummaria, and Pinna* sp.) that, today, are characteristic inhabitants of inner to middle shelf muddy soft-grounds (Marasti, 1991; Bernasconi and Robba, 1993). Sediment grain size, complete biogenic homogenisation, and macrofossil content converge to indicate that this mudstone-rich facies association has been deposited between fair-weather and storm-wave base and reflects accumulation in an offshore-transition depositional environment. The high degree of bioturbation observed in this facies association indicates that storm events were likely followed by long periods of low-energy conditions favoring the intense reworking of sediments.

Upper shoreface to foreshore cross- and plane-parallel laminated sandstones (UShFo)

This facies association is in the upper part of $Qm2_2$ and is about 6 m-thick, composed of medium- to coarse-grained sandstone beds with swaley cross-stratification in the lower part, plane-parallel laminated and high-angle trough and planar cross-bedded sandstones in sets several tens of centimeters thick in the middle part, and plane-parallel laminated sandstones in wedge-shaped sets dipping seaward at low angles in the uppermost part. Due to intense bioturbation by rootlets, the uppermost 1.5 m of this facies association is usually massive, with the root traces subtending from a laterally extensive, planar top surface associated with a reddish palaeosol (Fig. 2D). Palaeocurrent measurements in high-angle planar cross-beds indicate a dominant southeastward flow direction. Local patches displaying intense reworking by large *Macaronichnus*, with horizontal burrows generally running parallel to the bedding planes account for most of the bioturbation in this facies association.

The lower boundary of this sandstone package is sharp, typically flat and erosional onto the underlying mud-rich sediments (Fig. 2C), whereas the upper boundary is a surface of subaerial exposure, typically marked by a rooted, reddish paleosol (Fig. 2D). About 5 km southeast of the Torre Mucchia Section, well preserved within this subaerially weathered horizon, Agostini et al. (2007) documented a

vertebrate fossil fauna including the hippopotamus *Hippopotamus* ex gr. *H. antiquus*, the straight-tusked elephant *Elephas* (*Loxodon*) *antiquus*, and the red deer *Cervus elaphus*.

Swaley cross-stratification (Leckie and Walker, 1982) is usually associated to the combination of powerful storm-generated unidirectional and oscillatory flows at and above the limit of the fair-weather wave base (e.g. Dott and Bourgeois, 1982; Arnott, 1992). Planar and trough cross-stratification denotes migration of two- and three-dimensional dunes. The abundance of shoreline-parallel paleocurrents implies that strong longshore currents transported large volumes of sand (e.g., Hart and Plint, 1989; Walker and Plint, 1992; Frébourg et al., 2012). The relatively low intensity of bioturbation and impoverished ichnological diversity together with the preserved sedimentary structures are indicative of deposition in a storm/wave influenced shoreface environment, in which high storm-wave frequency and energy resulted in amalgamated sandstone beds (e.g., Burgeois and Leithold, 1984; Clifton and Dingler, 1984; Church and Middleton, 2003). In this setting, both two- and three-dimensional dunes migrated episodically, as evidenced by the local occurrence of completely bioturbated bedding planes, which represent periods of colonization of a shifting sandy substrate by polychaete worms. The seaward-dipping, low-angle, plane-parallel laminated sandstones in the uppermost part of this facies association are interpreted as foreshore deposits where plane-parallel-lamination formed under upper flow regime due to intense swash and backwash processes. This interpretation is supported by the occurrence of root traces and a capping paleosol representing a period of sub-aerial exposure and pedogenic alteration of the deposits. This sharp-based, regressive succession indicates limited accommodation in front of the prograding shoreface and represents a relative drop in sea level. Accordingly, it is placed in the falling stage systems tract and its erosional base is interpreted as a regressive surface of marine erosion.

Palustrine chalky carbonates (Pal)

This facies association, up to 0.5 m in thickness, characterizes the lowermost portion of $Qm2_1$ and shows an unconformable lower boundary with the underlying upper shoreface-foreshore sandstones, highlighted by the occurrence of a rooted red paleosol (Fig. 2D). The facies association consists of chalky carbonates and includes three main facies, namely A, B, and C (Fig. 3A), composed of

intensively rooted wackestone, packstone, grainstone and mudstone beds, rich in gastropods, intraclasts, calcareous and siliciclastic sand.

The basal facies A (Fig. 3B) is composed of fine to medium packed sands (7.5YR 8/3) with abundant blackish to reddish Fe/Mn precipitation features along irregular wavy sub-horizontal laminae and by reddish to orange (5YR 4/2) sub-vertical features that cross the laminated sands (Fig. 3B). Macro- and micromorphological observations do not reveal any carbonate leaching or clay illuviation features. The basal surface of this facies is also characterized by the presence of strongly cemented, cylindrical root traces (Fig. 3C). Two main microfacies can be recognized, namely A-1 and A-2. The basal A-1 microfacies (Fig. 4A) is made up of packed sands (c/f ratio 1), with light micritic groundmass and very abundant blackish impregnation features scattered or roughly aligned along undulated, irregular sub-horizontal surfaces. The coarse fraction is composed of predominant subangular to angular chert and quartz grains with subordinated rounded to subrounded limestone grains. An abrupt change marks the appearance of the upper A-2 microfacies. The coarse fraction decreases (c/f ratio 1/10), the groundmass is darker and made of cyanobacterial clotted micrite (Fig. 4B). Fe/Mn features concentrate along voids, cracks or diffused in the groundmass with dendrolithic forms (Fig. 4C). Microsparitic or sparitic features are rare and mainly related to dissolution of shells or as coatings of small biological voids.
A clear undulated boundary marks the transition to the overlying facies B (Fig. 3A), which is characterized by a weak lamination, abundant presence of gastropods, common fine and thin vertical tubules, abundant yellowish-orange to reddish- black Fe/Mn masses, nodules or concentrations within the vertical tubules. A single microfacies is recognized in facies B, with a c/f ratio 1/4 and decreasing Fe/Mn features toward the top. These are coatings and infillings of planes, voids and cracks (Fig. 4D), locally with precipitation of hematite, and quasi-coatings around voids and impregnative masses within the groundmass. The groundmass is dominated by cyanobacterial clotted dark micrite irregularly alternated with lighter micrite. Microsparite and sparite are rare, related to dissolution of shells or as coatings on rounded biological voids (Fig. 4E).

A diffused boundary separates facies B from the overlying muddy facies C (Fig. 3A). The color of facies C is lighter (10YR 8/2), thin vertical root traces filled with yellowish orange silts are commons (Fig. 3D); Fe/Mn features are scarce whereas large $CaCO_3$ nodules or irregular concentrations are

common and gastropods are abundant (Fig. 3D) and include a mixture of terrestrial pulmonates and freshwater prosobranchs (*Viviparus* sp., *Cepaea* sp., *Valvata* sp., and *Bithynia* sp.; D. Esu, 2014 and M. Magnatti, 2016 personal communications). Microfacies C-1 is observed at the base. This is dominated by irregularly distributed dark cyanobacterial clotted micrite (Fig. 4F) with very abundant shells, shell fragments and foraminifera. The coarse mineral fraction is subordinated (c/f ratio 1/8). Orange to reddish Fe precipitation features are concentrated within planes, cracks and biological voids (Fig. 3E). Microsparitic and sparitic features are very rare, fine and mostly related to dissolution of shells. Toward the top the microfacies progressively changes into the Microfacies C-2, characterized by irregularly alternating dark cyanobacterial clotted micrite and light micrite dominated groundmass (Fig. 4G). The darker cyanobacterial micrite is also characterized by abundant microsparitic and sparitic fillings and coatings along cracks and biological voids (Fig. 4H). Fe/Mn features are scarce and made of small nodules and impregnative features that are more abundant within the darker groundmass patches.

This facies association represents marl prairie palustrine carbonates precipitated both biogenically and physico-chemically within very shallow carbonate marshes in seasonal freshwater wetlands (e.g. Platt and Wright, 1992; Alonso-Zarza et al., 2006; MacNeil and Jones, 2006; Reuter et al., 2009) that were characterized by slowly moving or stagnant water. Macro- and micromorphological observations indicate that the rooted paleosoil that developed on top of the marine sands represents a short-lived event of exposure, lacking any evidence of weathering of the mineral fraction, carbonate leaching and clay neoformation or illuviation. The main observed processes are related to a vadose environment, typically cyanobacterial clotted micrite alternated with light micrite. The rare microsparitic coatings and fillings suggests very short-lived periods of complete subaerial exposure. However, phreatic cements are very rare, more abundant in the upper facies suggesting the rising of the water table and the possible flooding of the environment. Water table oscillation in vadose environment is also indicated by the abundance of Fe/Mn features (marmorization, *sensu* Freytet and Verrecchia, 2002).

Lagoon interbedded grey-green mudstones and very fine-grained sandstones (Lg)

This facies association forms the bulk of $Qm2_1$ and is between 15 m and 18 m thick, of which only the basal 8 m are continuously exposed in the studied section. This sediment package consists of organic-

rich (essentially plant debris), grey to green massive mudstones interbedded with subordinate, decimetric- to centimetric-thick, very fine-grained sandstone beds showing no overall grain-size trends. Traces of bioturbation and scattered mollusk shells are found throughout the sampled interval.

A distinctive, 0.4 m-thick, highly-fossiliferous horizon occurs at the top of the exposed section and represents the richest source of paleontological data, yielding abundant mollusks, fishes, benthic meiofauna, and planktonic foraminifers. The mollusk assemblage consists of the macromollusk *Cerastoderma glaucum* (mainly represented by juvenile individuals) and *Abra segmentum* along with a slightly more diverse micromollusk group including extremely abundant hydrobiid mudsnails, *Bittium scabrum*, *Planorbarius corneus*, *Rissoa membranacea*, *Theodoxus fluviatilis*, *Tragula fenestrata* and *Valvata piscinalis* (Fig. 5). Most of the faunal components are relatively well preserved and a minor amount of shells show a poor state of preservation.

The vertebrate assemblage is composed of fish remains, including saccular otoliths and a few teeth (Fig. 6). The fish otoliths are scarcely diversified, revealing a remarkable oligotypic character of the fish assemblage. About 75% of the recognized specimens belong to the big-scale sand smelt *Atherina hepsetus*. The remaining part of the assemblage is represented by gobies morphologically very similar to those pertaining to the *Pomatoschistus minutus* species complex (see Webb, 1980; Nolf, 2013). The ostracod fauna exhibits the overwhelming dominance of the highly euryhaline *Cyprideis torosa* and a few scattered valves of *Leptocythere* sp. accompanied by a benthic foraminiferal fauna characterized by an oligotypic assemblage dominated by the euryaline species *Ammonia beccarii* (about 80%) and subordinately by *Haynesina paucilocula* (10%), *Valvulineria perlucida* (7%) and *Cribrononion granosum* (3%) (Fig. 7). The samples contain mostly reworked benthic and planktonic foraminifers, usually poorly preserved, with eroded and broken shells. Reworked benthic foraminifers belong to the following taxa: *Hyalinea baltica*, *Elphidium crispum* and *Cibicides* sp., whereas the planktonic foraminifers, usually very small in size, are *Globorotalia inflata*, *Globigerinoides* sp., and *Globorotalia* sp.

The rich organic fraction suggests deposition in a low-energy, restricted, brackish-water, lagoonal environment occasionally affected by high-energy events represented by back-barrier overwash sandstone beds.

Monospecific ostracod assemblages dominated by *C. torosa* are interpreted to represent environmental stress. This species is typical of brackish-water and lagoonal environments (Athersuch et al., 1989; Meisch, 2000) and it is also highly euryhaline, showing an adaptability to salinities from 0.4 to 150‰ (Neale, 1988) and therefore an opportunistic behavior (Frenzel and Boomer, 2005). The comparison between the abundance of the species *A. beccarii* with those of the species *H. paucilocula*, *V. perlucida* and *C. granosum* suggests the presence of distinct lagoonal environments (Albani and Serandri-Barbero 1982; Serandrei-Barbero et al., 2005, 2006; Zecchin et al., 2009). In this case, a high percentage of *A. beccarii* and a low abundance of *H. paucilocula*, *V. perlucida* and *C. granosum* identify an inner lagoonal environment with hyposaline conditions (Albani and Serandrei Barbero, 1982; Donnici et al., 1997; Serandrei-Barbero et al., 2005, 2006).

The mollusk record is characterized by some brackish-water taxa (among which Hydrobiidae, *A. segmentum* and *C. glaucum*, in order of abundance) typical of the euryhaline and eurythermal lagoons (LEE *sensu* Peres and Picard, 1964). Hydrobiidae are herbivores or surface detritivores burrowers adapted to euryhaline conditions ranging from 2 to 34‰ even if usually they prefer the range 6-25‰ (Fretter and Graham, 1978), *C. glaucum* is a filter-feeder normally living in water bodies characterized by salinities between 18 and 37‰ (Vatova, 1981), and *A. segmentum* is a browser-burrower which thrives in a salinity range of 14-27‰. Therefore the contemporaneous occurrence of these three taxa might suggest a range of salinity between 18 and 27‰. However, the presence of *P. corneus*, *V. piscinalis*, a fresh-water species which tolerates slightly brackish waters (Grigorovich et al., 2005), and of *R. membranosa*, which regularly occurs at salinities of 7–10‰ (Waren, 1996), along with the absence of marine affinity taxa point toward mesohaline waters far from marine influence. This is not in contrast with the presence of *A. segmentum* and juvenile individuals of *C. glaucum* because these taxa may tolerate low salinities as low as 5‰ (Di Rita et al., 2011), a value considered as a critical threshold for distribution of the lagoonal taxa (Cognetti and Maltagliati, 2000). Data from the mollusk content are consistent with a low-energy brackish environment with very limited marine influence, such as an inner lagoon, in which the presence of algal/plant meadows is suggested by the occurrence

of browsers. According to the "confinement model" proposed by Guelorget and Perthuisot (1992) the paralic mollusk assemblage may be referable to a lagoon environment of zone IV corresponding to a rather high degree of confinement. Such a zonal reference is supported also by the sketch proposed by Breber et al. (2000) solely based on bivalves.

Sand smelts and gobies are common constituents of paralic assemblages in terms of relative abundance, representing among the best adapted fishes for this type of habitats (e.g., Harrison and Whitfield, 1995). Sand smelts are small-sized pelagic planktivores that usually reside in paralic biotopes in which they can complete their short life cycles (e.g., Nordlie, 2003; Franco et al., 2006). More particularly, *Atherina hepsetus* exhibits a strong tolerance to broad salinity variations, inhabiting waters with salinities ranging from 1.6 to 4.5‰ (Kiener and Spillmann, 1969). Gobies of the genus *Pomatoschistus* are very abundant in shallow coastal areas, estuaries, coastal lagoons and marine bays of the Mediterreanean and Eastern Atlantic Ocean were they feed on small benthic invertebrates, pelagic copepoda and small fishes (e.g., Hamerlynck and Cattrijsse, 1994). From an ecological point of view, all the recognized fish taxa can be assigned to the guild of estuarine residents (see Elliot and Dewailly, 1995), which includes species that spend their life in brackish biotopes influenced by marine waters. Overall, the exclusive presence of taxa belonging to this guild is indicative of soft bottoms and densely vegetated biotopes (Paterson and Whitfield, 2000). The absence of marine and/or freshwater migratory species seems to be indicative of the reduced influence of both the marine inflow and freshwater outflow, suggesting that the original depositional environment was characterized by a relatively high degree of confinement (Zones III and IV of the confinement scale of Guelorget and Perthuisot, 1992).

Pollen analysis

The pollen record of the Torre Mucchia section shows the development of a forest vegetation dominated by *Pinus* (>40%), accompanied by a number of mesophilous and thermophilous tree taxa, including deciduous and evergreen *Quercus*, reaching 13 and 9%, respectively, *Alnus* (8%), *Carpinus orientalis* type (7%), *Carpinus betulus* (2%), *Picea* (7%), *Juniperus* (7%), *Abies* (6%), and several other tree taxa in low percentages (Fig. 8). A significant presence of *Tsuga* pollen, attaining 9% in one sample, *Carya*, reaching values of 5% in the bottom samples, and *Zelkova* (12%), accompanied by scattered presence of *Pterocarya*, are of special interest, as these tree taxa disappeared from Europe in

the course of the Middle Pleistocene (Bertini, 2010; Magri and Palombo, 2013). Chenopodiaceae (max. 30%), *Artemisia* (17%), Cichorioideae (15%), Asteroideae (6%), Poaceae (13%), and Apiaceae (7%) are common herbaceous taxa throughout the record.

As a whole, the pollen record represents an open forest, whose floristic composition clearly reflects a mixture of both mountain (Majella Massif) and coastal (Adriatic Sea) environments and suggests that a variety of vegetation belts were present in the surrounding areas: i) a mountain belt that includes high-altitude, water-demanding trees, such as *Picea*, *Abies*, *Tsuga*, and *Betula*; ii) a mid-altitude belt including *Carya*, *Carpinus*, deciduous *Quercus*, *Alnus*, and *Corylus*; and iii) a warm coastal belt including evergreen *Quercus* and possibly *Zelkova*. The percentage values of Asteraceae (between 6% and 32%) and Apiaceae (up to 7%) indicate the presence of wide open areas dominated by steppe elements. Together with the abundance of *Pinus*, they suggest that the recorded environments do not represent the fully developed forest conditions that correspond to the warmest and wettest phases of interglacial periods, which are generally dominated by broadleaved trees. The continuous and significant frequencies of chenopods suggest saline conditions linked to the proximity of the sea, as also indicated by the presence of foraminiferal linings and dinocysts. Similar conditions were recorded in other pollen diagrams from coastal environments, in connection with inputs of marine water into coastal lakes (Di Rita and Melis, 2013; Melis et al., 2015).

Discussion

Stratigraphic evolution

In the studied section, the vertical succession of facies associations can be interpreted as related to relative sea-level oscillations and comprises the two youngest sequences exposed in the Ortona area, namely $Qm2_2$ and $Qm2_1$ (Fig. 2C). The lower sequence ($Qm2_2$) includes a transgressive, deepening- and fining-upward shoreface to offshore-transition facies succession overlain by a shoreface-foreshore body with an erosive base and a rooted pedogenic horizon at the top (Di Celma et al., 2016a). The presence at the base of the shoreface-foreshore sandstones of a sharp and scoured surface that truncates to some degree the underlying offshore-transition sediments and the evidence of subaerial exposure and pedogenic modification at its top imply forced regression and deposition during sea-level fall (Plint and

448 Nummedal, 2000 and references therein). The degree of development of paleosols is function of the
449 soil-forming factors that in sedimentary record i.e., regressive-trasgressive cycles, can be summarized
450 into time (length of subaerial exposure of the surface; Kraus, 1999) and climate conditions (Interglacial
451 vs. Glacial; Coltorti and Pieruccini, 2006). The weakly developed interfluve palaeosol described here
452 can be traced laterally into the basal erosional surface of an incised valley fill (Di Celma et al., 2016a)
453 and, therefore, it is interpreted to represent a sequence-bounding subaerial unconformity. In forced
454 regressive stages subaerial unconformities are highly diachronous surfaces that form initially in updip
455 areas and gradually expand in a basinward direction as the sea-level falls and the shoreline regresses
456 (e.g., Plint et al., 2001). The paleosols development continues during subsequent lowstand normal
457 regression and transgression and does not cease until the exposure surface becomes buried by renewed
458 deposition. These observations imply that the degree of development of sequence-bounding interfluve
459 paleosols is a function of their position along the depositional profile, with the most mature paleosols
460 predicted in the most updip areas and the least developed paleosols expected to form in the most
461 downdip areas, where they have less time to develop. As a result, the poorly developed character of the
462 paleosol exposed at Torre Mucchia can be interpreted as reflecting a distal position of the study section
463 along the subaerially exposed shelf. Moreover, the described paleosol formed during an eustatic forced
464 regression and, therefore, not in fully Interglacial conditions, when long lasting warm and wet climatic
465 conditions favor the formation of strongly developed paleosols as observed also in the nearby areas
466 (Coltorti and Pieruccini, 2006; Di Celma et al., 2015). These would not only explain the low degree of
467 pedological development of the paleosol, but also the abundance of *Pinus* and herbs in the pollen
468 record from the lagoon mudstones, reflecting the initial transgression during a glacial-interglacial
469 transition, as also recorded in other lagoon sites (Di Rita et al., 2015). High percentage values of *Pinus*,
470 generally >30%, accompanied by deciduous trees not exceeding 10%, characterized also the
471 interglacial vegetation of the Cesi section, an early Middle Pleistocene pollen site in central Italy
472 (Bertini, 2000). During the subsequent transgression, the landward migration of a barrier-lagoon
473 system developed behind the transgressing shoreline resulted in the inundation of the previous coastal
474 plain and deposition of palustrine carbonates in a freshwater coastal wetland that eventually evolved
475 into a brackish lagoon within which mud-rich sediments were deposited.
476
477 *Chronological constraints*

The compositional correlation between the pollen assemblage retrieved from the lagoon mudstones of the $Qm2_1$ sequence and other floristic records documented in central-southern Italy, between 42° and 39° latitude N (Figs. 1A, 9), provides some additional chronological constraint for the studied succession. *Tsuga*, reaching the significant percentage of 9% at Torre Mucchia, was found in appreciable amounts (>5%) until MIS 18 at Montalbano Jonico, a sequence dated by means of two $^{40}Ar/^{39}Ar$ ages on volcaniclastic layers ($^{40}Ar/^{39}Ar$ 773.9 ± 1.3 and 801.2 ± 19.5 ka; Bertini et al., 2015). It was also continuously found at Valle di Manche before and soon after the Matuyama–Brunhes boundary (Capraro et al., 2005). After that time, *Tsuga* was found in two levels (<2.5%) in the deposit of Sessano, correlated with MIS 13 on the basis of a $^{40}Ar/^{39}Ar$ age (437.9 ± 1.9 ka; Russo Ermolli et al., 2010). During the same interglacial, there are only two occurrences of single grains at Vallo di Diano (Russo Ermolli, 1994). Other pollen records from southern Italy correlated with MIS 13 (Acerno, Boiano and Mercure; Russo Ermolli et al., 2015) do not record any pollen grain of *Tsuga* and indicate that its range was markedly fragmented, as it is expected for a tree population that is undergoing extinction. On the whole, the abundance of *Tsuga* in the $Qm2_1$ sequence suggests an age older than MIS 16 (Fig. 9).

Another tree taxon that is no longer present in Italy is *Carya*, which is very abundant (>25%) in central Italy during the Early Pleistocene interglacials between 1.8 and 1.2 Ma (Magri and Palombo, 2013). Percentages <10% have been documented at Fontana Ranuccio, in sediments underlying the Matuyama–Brunhes boundary and ascribed to MIS 21 (Corrado and Magri, 2011). During MIS 19, at Montalbano Jonico (Bertini et al., 2015) and Valle di Manche (Capraro et al., 2005) *Carya* never reached values >5%. *Carya* was absent from Vallo di Diano during MIS 15, but continuously present in very low abundance during MIS 13 (Russo Ermolli, 1994). Pollen associated to a macrofossil find dated 530 ka at Carsoli (Sadori et al., 2010) and pollen grains (always <1.5%) at Ceprano (Manzi et al., 2010) confirm its presence in Central Italy during MIS 13. The very last appearances of *Carya* are documented at Boiano, southern Italy, within MIS 9 sediments (Orain et al., 2013). The pollen record from the $Qm2_1$ sequence, showing maximum values of *Carya* around 5%, fits the progressive reduction of this taxon during the Middle Pleistocene, further supporting an age older than MIS 16 for the Torre Mucchia pollen record (Fig. 9).

On the whole, the pollen diagram from the Middle Pleistocene lagoon mudstones of the $Qm2_1$ sequence is similar to the records correlated with MIS 21–17, while it is clearly distinct from the records corresponding to MIS 15–13 (Fig. 9). This attribution is also supported by the presence of *Pterocarya*, whose appearances become sporadic in the records corresponding to MIS 15–13 (Fig. 9). In contrast, *Carpinus* and *Fagus*, showing low percentages in all the Italian records between 1.5 and 0.7 Ma (Magri and Palombo, 2013), increase to values of 5–10%, in correspondence with high percentages of *Abies*, during MIS 15 and 13 (Fig. 9). The difference in vegetation between MIS 21–17 and MIS 15–13 is also marked by the reduction of *Tsuga* and *Carya*. This turnover in the composition of forest vegetation may be explained by the extreme climatic conditions of MIS 16 (Tzedakis et al., 2006).

The correlation of the mammal assemblage from the immediately underlying paleosol to an interval bracketed between MIS 19 and MIS 17 (Mazza and Bertini, 2013), based on the paleomagnetic reversal assigned to the Matuyama-Bruhnes transition in the nearby section of Ortona (Agostini et al., 2007), provides an additional chronological constraint, as it implies an age younger than MIS 19. Thus, it is feasible that the studied portion of the $Qm2_1$ sequence was laid down during the early transgression of MIS 17, not in fully interglacial conditions yet.

Conclusions

The multi-disciplinary analysis carried out on the Torre Mucchia section, Ortona, integrates sedimentological features with data obtained from the analysis of fish, mollusks, pollen, ostracods and foraminifers found within the sedimentary section. These data provide a rare opportunity to reconstruct the articulate evolutionary scenario of a coastal area along the western side of the Adriatic Sea during Middle Pleistocene and a constraint for the age of the upper part of the Qm2 Unit ($Qm2_1$ sequence). The stratigraphic unconformity at the top of the forced regressive upper shoreface-foreshore sandstones, marked by a rooted reddish paleosol, records a phase of non-deposition and pedogenic modification in the study area. Above this emerged surface, the palustrine carbonates represent the first record of transgressive deposition and the transgressive surface is located at its lower boundary, at the passage with the underlying rooted paleosol. Sedimentological, paleontological and micromorphological features suggest that these carbonates were deposited within very shallow,

seasonal freshwater wetlands probably developed not far from the coeval coastline. As relative sea-level rise and transgression proceeded, the freshwater wetlands evolved into a brackish lagoon in which mud-rich sediments were deposited. The paleontological content and composition of the pollen assemblage provide useful information about the palaeoenvironmental and climatic conditions along the western Adriatic Sea during deposition of the $Qm2_1$ sequence and a valuable clue to the chronostratigraphy and geochronology of the studied section. Within these deposits, the faunal assemblages suggest that the original depositional environment was characterized by brackish waters and a relatively high degree of confinement. The pollen record documents the development of a forest vegetation dominated by *Pinus* and accompanied by a number of mesophilous and thermophilous tree taxa and significant amounts of herbaceous pollen pointing to the presence of wide open areas. These vegetation features, considered in the light of the correlation with the mammal fauna and the paleomagnetism of a nearby sequence from Ortona (Agostini et al., 2007; Mazza and Bertini, 2013), are suggestive of deposition during an early phase of MIS 17.

The new pollen record from Torre Mucchia fills a gap of information on the vegetation history in Central Italy, thus significantly improving our understanding of the vegetation development during the Middle Pleistocene and especially of the role played by the most marked glacial periods in determining the reduction or disappearance of tree taxa that are nowadays extinct in the Italian Peninsula.

Acknowledgments

Journal reviewers Jan Henninsen and Alessandro Amorosi, Associate Editor John Dodson and Editor Lewis Owen are gratefully acknowledged for their constructive reviews and helpful criticism that sharpened the focus of this study. The research of CDC was supported by grants (FAR 2013, 2014) of the Università degli Studi di Camerino. The research of GC was supported by grants (ex-60% 2015) of the Università degli Studi di Torino.

Figure captions

Figure 1. (A) Location map of Ortona and the main Middle Pleistocene Italian sites (between ca. 39° and 42° N) cited in the text for their palynological data. (B) Enlarged satellite image showing location of the study area.

Figure 2. (A) Panoramic view of the Torre Mucchia section. Dashed and dotted lines as indicated in C. (B) Detail of the shell-rich interval embedded in the lagoon mudstones. (C) Vertical distribution of facies associations and sequence stratigraphic interpretation of the studied section. The key stratal surfaces are highlighted by dashed and dotted lines. LSh, lower shoreface; OfTr, offshore-transition; UShFo, upper shoreface-foreshore; Lg, lagoon mudstones. (D) View of outcrop showing the vertical transition from sequence $Qm2_2$ to sequence $Qm2_1$. UshFo, upper shoreface-foreshore sandstones; Ps, paleosol; Pal, palustrine carbonates; Lg, lagoon mudstones.

Figure 3. Compilation of field photographs showing the main sedimentological characteristics of palustrine carbonates. (A) The facies of the palustrine carbonates as visible at the scale of the outcrop and on thin section. (B) Reddish Fe-precipitation features along the root-tracks across the laminated sandstones. The black wavy laminae follow Fe-Mn precipitation along sedimentary structures and mark small changes in grain-size. (C) The root tracks on the lower surface marked by stronger cementation. Locally, small voids are still present (indicated by arrows). (D) Remnants of vertical root traces (white arrows) and gastropods (black arrows). (E) Plain view of the upper surface characterized by Fe precipitation and coating around the root-traces.

Figure 4. Micromorphological features of palustrine carbonates. (A) Microfacies A-1: packed sands with micritic groundmass made of predominant subangular to angular chert and quartz grains with subordinated rounded to subrounded limestone grains (XPL). (B) Microfacies A-2: groundmass made of dark cyanobacterial clotted micrite (PPL). (C) Microfacies A-2: abundant Fe/Mn precipitation features also with dendrolitic forms (PPL). (D) Microfacies B: sub-horizontal planar voids filled with Fe/Mn features, more frequent toward the top, and impregnation features and masses in the dark cyanobacterial clotted micrite of the groundmass (PPL). (E) Microfacies B: characters of the patches of lighter micritic groundmass with rare microsparitic and sparitic features mainly related to dissolution of shells or as coatings on biological voids (PPL). (F) Microfacies C-1: overall aspect with dark cyanobacterial clotted micrite and very abundant shells, shell fragments and foraminifera (PPL). (G) Microfacies C-2: the alternating patches of dark cyanobacterial clotted micrite and light micrite in the groundmass (PPL). (H) The darker patches

of cyanobacterial micrite with abundant microsparitic and sparitic fillings of cracks and biological voids (XPL)

Figure 5. Mollusks from the Middle Pleistocene lagoonal mudstones exposed at Torre Mucchia. Vertical bars 2 mm; Horizontal bar 4 mm. (A-B) *Planorbarius corneus*. (C-D) *Theodoxus fluviatilis*. (E-F) *Valvata piscinalis*. (G) *Rissoa membranacea*. (H) *Ecrobia ventrosa*. (I) *Cerastoderma glaucum*. (J) *Abra segmentum*.

Figure 6. Fish otoliths from the Middle Pleistocene lagoonal mudstones exposed at Torre Mucchia. (A) *Atherina hepsetus* Linnaeus, 1758. (B) *Pomatoschistus* aff. *minutus* (Pallas, 1770).

Figure 7. Microphotographs of the main biogenic content of lagoon sandy mudstones. Scale bars 1 mm. (A) Sample 3ORT, vegetal remains, *Ammonia beccarii* (a), limonite nodules (b) and framboidal pyrite (c). (B) Sample 3ORT, *Cribrononion granosum* (a), *Valvulineria perlucida* (b) and framboidal pyrite (c). (C) Sample 4ORT, biogenic detritus with *Haynesina paucilocula* (a); *Ammonia beccarrii* (b). (D) Sample 4ORT, biogenic detritus with *Ammonia beccarii* (a), *Valvulineria perlucida* (b); *Haynesina paucilocula* (c); *Cyprideis torosa* (d).

Figure 8. Pollen percentage diagram of the Torre Mucchia section.

Figure 9. Stratigraphic setting of selected Early and Middle Pleistocene pollen records from the Italian Peninsula (42°-39°latitude N), and schematic pollen biostratigraphy of selected pollen taxa (modified from Magri and Palombo, 2013).

References

Agostini, S., Bertini, A., Caramiello, S., De Flavis, A.G., Mazza, P., Rossi, M.A., Satolli, S., 2007. A new mammalian bone bed from the lower Middle Pleistocene of Ortona (Chieti, Abruzzo, central Italy). In: Coccioni, R., Marsili, A. (Eds.), Proceedings of the Giornate di Paleontologia 2005, vol. 12. Grzybowski Foundation, pp. 1–5.

Aguirre, J., de Gibert, J.M., Puga-Bernabéu, A., 2010. Proximal–distal ichnofabric changes in a siliciclastic shelf, Early Pliocene, Guadalquivir Basin, southwest Spain. Palaeogeography Palaeoclimatology Palaeoecology 291, 328–337.

Albani, A.D., Serandrei-Barbero, R., 1982. A foraminiferal fauna from the lagoon of Venice, Italy. Journal of Foraminiferal Research 12, 234–241.

Alonso-Zarza, A.M., Dorado-Valiño, M., Valdeolmillos-Rodríguez, A., Ruiz-Zapata, M.B., 2006. A recent analogue for palustrine carbonate environments: The Quaternary deposits of Las Tablas de Daimiel wetlands, Ciudad Real, Spain. GSA Special Papers 416, 153–168.

Alonso-Zarza, A.M., Wright, V.M., 2010. Palustrine carbonates. In: Alonso-Zarza, AM., Tanner, L.H. (Eds.). Carbonates in Continental Settings: Facies. Environments and Processes. Developments in Sedimentology, 61, Elsevier, Amsterdam, pp. 103–132.

Amorosi, A., Bracone, V., Di Donato, V., Rosskopf, C.M. and Aucelli, P.P.C., 2009. The Plio-Pleistocene succession between Trigno and Fortore rivers (Molise and Apulia Apennines): stratigraphy and facies characteristics. GeoActa 8, 1–12.

Amorosi, A., Pacifico, A., Rossi, V. Ruberti, D., 2012. Late Quaternary incision and deposition in an active volcanic setting: The Volturno valley fill, southern Italy. Sedimentary Geology 282, 307–320.

Amorosi, A., Rossi, V., Vella, C., 2013. Stepwise post-glacial transgression in the Rhône Delta area as revealed by high-resolution core data. Palaeogeography, Palaeoclimatology, Palaeoecology 374, 314–326.

Arnott, R.W.C., 1992. Ripple cross-stratification in swaley cross-stratified sandstones of the Chungo Member, Mount Yamnuska, Alberta. Canadian Journal of Earth Sciences 29, 1802–1805.

Artoni, A., 2013. The Pliocene-Pleistocene stratigraphic and tectonic evolution of the Central sector of the Western Periadriatic Basin of Italy. Marine and Petroleum Geology 42, 82–106.

Athersuch, J., Horne, D.J., Whittaker, J.E., 1989. Marine and brackish water ostracods. Leiden: E.J. Brill, 343 pp. Synopses of the British fauna, New Series, no. 43.

Bennett, K., 2009. “psimpoll”and “pscomb”: C programs for analysing pollen data and plotting pollen diagrams (version 4.27). Available online from Queen’s University Quaternary Geology program at URL http://www. chrono. qub. ac. uk/psimpoll. html.

Bernasconi, M.P., Robba, E., 1993. Molluscan palaeoecology and sedimentological features: an integrated approach from the Miocene Meduna section, northern Italy. Palaeogeography, Palaeoclimatology, Palaeoecology 100, 267–290.

Bertini, A., 2000. Pollen record from Colle Curti and Cesi: early and middle Pleistocene mammal sites in the Umbro–Marchean Apennine mountains (central Italy). Journal of Quaternary Science 15, 825–840.

Bertini, A., 2010. Pliocene to Pleistocene palynoflora and vegetation in Italy: State of the art. Quaternary International 225, 5–24.

Bertini, A., Toti, F., Marino, M., Ciaranfi, N., 2015. Vegetation and climate across the Early–Middle Pleistocene transition at Montalbano Jonico, southern Italy. Quaternary International 383, 74–88.

Bigi, S., Conti, A., Casero, P., Ruggiero, L., Recanati, R., Lipparini, L., 2013. Geological model of the central Periadriatic basin (Apennines, Italy). Marine and Petroleum Geology 42, 107–121.

Bourgeois, J., Leithold, E.L., 1984. Wave-worked conglomerates — Depositional processes and criteria for recognition. In: Koster, E.H., Steel, R.J. (Eds.), Sedimentology of Gravels and Conglomerates. Canadian Society of Petroleum Geologists Memoirs 10, 331–343.

Bracone, V., Amorosi, A., Aucelli, P.P.C., Ciampo, G., Di Donato, V., Rosskopf, C.M., 2012a. Palaeoenvironmental evolution of the Plio-Pleistocene Molise Periadriatic Basin (Southern Apennines, Italy): insight from Montesecco Clays. Ital. J. Geosci. (Boll. Soc. Geol. It.) 131, 272–285.

Bracone, V., Amorosi, A., Aucelli, P.P.C., Rosskopf, C.M., Scarciglia, F., Di Donato, V., Esposito, P. 2012b. The Pleistocene tectono-sedimentary evolution of the Apenninic foreland basin between Trigno and Fortore rivers (Southern Italy) through a sequence-stratigraphic perspective. Basin Research 24, 213–233.

Breber P., Scirocco T., Cilenti L., 2000. An assessment of the fishery polential of Lesina lagoon (S. Italy) based on the composition and zonation of the macrobenthic fauna. Periodicum Biologorum, 102, Suppl. 1, 553–556.

Cantalamessa, G., Di Celma, C., 2004. Sequence response to syndepositional regional uplift: insights from high-resolution sequence stratigraphy of late Early Pleistocene strata, Periadriatic Basin, central Italy. Sedimentary Geology 164, 283–309.

Cantalamessa, G., Di Celma, C., Potetti, M., Lori, P., Didaskalou, P., Albianelli, A., Napoleone, G., 2009. Climatic control on deposition of upper Pliocene deepwater gravity-driven strata in the Apennines foredeep (central Italy): correlations to the marine oxygen sea isotope record. In: Kneller, B., Martinsen, O.J., McCaffrey, B. (Eds.), External Controls on Deep Water Depositional Systems: Climate, Sea-level, and Sediment Flux. SEPM Special Publication 92, 247–259.

Capraro, L., Asioli, A., Backman, J., Bertoldi, R., Channell, J.E.T., Massari, F., Rio, D., 2005. Climatic patterns revealed by pollen and oxygen isotope records across the Matuyama-Brunhes Boundary in

685 the central Mediterranean (southern Italy). Geological Society, London, Special Publications 247,
686 159–182.
687 Centamore, E., Nisio, S., 2003. Effects of uplift and tilting in the Central-northern Apennines (Italy).
688 Quaternary International 101–102, 93–101.
689 Church, M.J., Middleton, G.V., 2003. Encyclopedia of Sediments and Sedimentary Rocks. Springer-
690 Verlag, New York, 821 pp.
691 Clifton, H.E., Dingler, J.R., 1984. Wave-formed structures and paleoenvironmental reconstruction.
692 Marine Geology 60, 165–198.
693 Clifton, H.E., Thompson, J.K., 1978. *Macaronichnus segregatis*: a feeding structure of shallow marine
694 polychaetes. Journal of Sedimentary Petrology 48, 1293–1302.
695 Cognetti G., Maltagliati F., 2000. Biodiversity and adaptive mechanisms in brackish water fauna.
696 Marine Pollution Bulletin, 40, 7–14.
697 Coltorti, M., Pieruccini, P., 2006. The last interglacial pedocomplexes in the litho and morpho-
698 stratigraphical framework of the central-northern Apennines (Central Italy). Quaternary
699 International 156–157, 118–132.
700 Corrado, P., Magri, D., 2011. A late Early Pleistocene pollen record from Fontana Ranuccio (central
701 Italy). Journal of Quaternary Science 26, 335–344.
702 Di Celma, C., 2011. Sedimentology, architecture, and depositional evolution of a coarse-grained
703 submarine canyon fill from the Gelasian (early Pleistocene) of the Peri-Adriatic basin, Offida,
704 central Italy. Sedimentary Geology 238, 233–253.
705 Di Celma, C., Cantalamessa, G., 2012. Off-shelf sedimentary record of recurring global sea-level
706 changes during the Plio-Pleistocene: evidence from the cyclic fills of exhumed slope systems in
707 central Italy. Journal of the Geological Society, London 169, 643–646.
708 Di Celma, C., Cantalamessa, G., Didaskalou, P., 2013. Stratigraphic organization and predictability of
709 mixed coarse- and fine-grained successions in an upper slope turbidite system of the Peri-Adriatic
710 basin. Sedimentology 60, 763–799.
711 Di Celma, C., Cantalamessa, G., Didaskalou, P., Lori, P., 2010. Sedimentology, architecture, and
712 sequence stratigraphy of coarse-grained, submarine canyon fills from the Pleistocene (Gelasian-
713 Calabrian) of the Peri-Adriatic basin, central Italy. Marine and Petroleum Geology 27, 1340–1365.

714 Di Celma, C., Pieruccini, P., Farabollini, P., 2015. Major controls on architecture, sequence
715 stratigraphy and paleosols of middle Pleistocene continental sediments ("Qc Unit"), eastern central
716 Italy. Quaternary Research 83, 565–581.
717 Di Celma, C., Ragaini, L., Caffau, M., 2016a. Marine and nonmarine deposition in a long-term low-
718 accommodation setting: an example from the Middle Pleistocene Qm2 Unit, eastern Central Italy,
719 Marine and Petroleum Geology 72, 234–253.
720 Di Celma, C., Teloni, R., Rustichelli, A., 2016b. Evolution of the Gelasian (Pleistocene) slope turbidite
721 systems of southern Marche (Peri-Adriatic basin, central Italy). Journal of Maps 12, 137–151.
722 Di Rita, F., Melis, R.T., 2013. The cultural landscape near the ancient city of Tharros (central West
723 Sardinia): vegetation changes and human impact. Journal of Archaeological Science 40, 4271–
724 4282.
725 Di Rita, F., Celant, A., Milli, S., Magri, D., 2015. Lateglacial–early Holocene vegetation history of the
726 Tiber delta (Rome, Italy) under the influence of climate change and sea level rise. Review of
727 Palaeobotany and Palynology 218, 204–2016.
728 Di Rita, F., Simone, O., Caldara, M., Gehrels, W.R., Magri, D., 2011. Holocene environmental changes
729 in the coastal Tavoliere Plain (Apulia, southern Italy): A multiproxy approach. Palaeogeography,
730 Palaeoclimatology, Palaeoecology 310, 139–151.
731 Donnici, S., Serandrei-Barbero, R., Taroni, G., 1997. Living benthic foraminifera in the Lagoon of
732 Venice (Italy): population dynamics and its significance. Marine Micropaleontology 43, 440–454.
733 Dott, R.H., Jr., Bourgeois, J., 1982. Hummocky stratification: Significance of its variable bedding
734 sequences. Geological Society of America Bulletin 93, 663–80.
735 Durand, N., Monger, H.C., Canti, M.G., 2010. Calcium carbonate features. In: Stoops, G., Marcelino,
736 V. and Mees, F. (eds.), Interpretation of Micromorphological Features of Soils and Regoliths.
737 Elsevier, Amsterdam, pp. 149–194
738 Follieri, M., Magri, D., Sadori, L., 1988. 250000-year pollen record from Valle di Castiglione (Roma).
739 Pollen et Spores 30, 329–356.
740 Franco, A., Franzoi, P., Malavasi, S., Riccato, F., Torricelli, P., 2006. Fish assemblages in different
741 shallow water habitats of the Venice Lagoon. Hydrobiologia 555, 159–174.

742 Frébourg, G., Hasler, C.-A., Davaud, E., 2012. Uplifted marine terraces of the Akamas Peninsula
743 (Cyprus): evidence of climatic conditions during the Late Quaternary highstands. Sedimentology
744 59, 1409–1425.
745 Freytet, P., Verrecchia, E.P., 2002. Lacustrine and palustrine carbonate petrography: an overview.
746 Journal of Paleolimnology 27, 221–237.
747 Frenzel, P., Boomer, I., 2005. The use of ostracods from marginal marine, brackish waters as
748 bioindicators of modern and Quaternary environmental change. Palaeogeography,
749 Palaeoclimatology, Palaeoecology 225, 68–92.
750 Fretter, V., Graham, A., 1978. The Prosobranch Molluscs of Britain and Denmark. Part 3. Journal
751 Molluscan Studies, Suppl. 5, 101–151.
752 Ghielmi, M., Minervini, M., Nini, C., Rogledi, S., Rossi, M., 2013. Late Miocene-Middle Pleistocene
753 sequences in the Po Plain e Northern Adriatic Sea (Italy): The stratigraphic record of modification
754 phases affecting a complex foreland basin. Marine and Petroleum Geology 42, 50–81.
755 Grigorovich I.A., Mills E.L., Richards C.B., Breneman D., Ciborowski J.J.H., 2005, European valve
756 snail *Valvata piscinalis* (Muller) in the Laurentian Great Lakes Basin. Journal of Great Lakes
757 Research 31, 135-143.
758 Guelorget, O., Perthuisot, J.P., 1992, Paralic ecosystems: Biological organization and functioning. Vie
759 et Milieu 42, 215–251.
760 Gunderson, K.L., Pazzaglia, F.J., Picotti, V., Anastasio, D.J., Kodama, K.P., Rittenour, T., Frankel,
761 K.F., Ponza, A., Berti, C., Negri, A., Sabbatini, A., 2014. Unraveling tectonic and climatic controls
762 on synorogenic stratigraphy. Geological Society of America Bulletin 126, 532–552.
763 Hamerlynck, O., Cattrijsse, A., 1994. The food of *Pomatoschistus minutus* (Pisces, Gobiidae) in
764 Belgian coastal waters, and a comparison with the food of its potential competitor *P. lozanoi*.
765 Journal of Fish Biology 44, 753–771.
766 Harrison, T.D., Whitfield, A.K., 1995. Fish community structure in three temporarily open/closed
767 estuaries on the Natal coast. J.L.B. Smith Ichthyological Bulletin 64, 1–80.
768 Hart, B.S., Plint, A.G., 1989. Gravelly shoreface deposits: a comparison of modern and ancient facies
769 sequences. Sedimentology 36, 551–557.

Kaufman, D.S., 2000, Amino acid racemization in ostracodes, in Perspectives in Amino Acid and Protein Geochemistry (eds. G. Goodfriend, M. Collins, M. Fogel, S. Macko, J. Wehmiller), 145-160, Oxford University Press, New York.

Kaufman, D.S., 2006. Temperature sensitivity of aspartic and glutamic acid racemization in the foraminifera *Pulleniatina*. Quaternary Geochronology 1, 188–207.

Kiener, A., Spillmann, C.J., 1969. Contributions a l'étude systématique et écologique des athérines des cotes françaises. Mémoires du Muséum National d'Histoire Naturelle, Série A, Zoologie 60, 33–74.

Kraus, M.J., 1999. Paleosols in clastic sedimentary rocks: their geologic applications. Earth-Science Reviews 47, 41–70

Leckie, D.A, Walker, R.G., 1982. Storm- and tide-dominated shorelines in Late Cretaceous Moosebar-Lower Gates interval - outcrop equivalents of deep basin gas trap in western Canada. American Association of Petroleum Geologists Bulletin 66, 138–157.

Lisiecki, L.E., Raymo, M.E., 2005. A Pliocene-Pleistocene stack of 57 globally distributed benthic $\delta^{18}O$ records. Paleoceanography 20.

MacNeil, A.J., Jones, B., 2006. Palustrine deposits on Late Devonian coastal plain – sedimentary attributes and implications for concepts of carbonate sequence stratigraphy. Journal of Sedimentary Research 76, 292–309.

Magri, D., Palombo, M.R., 2013. Early to Middle Pleistocene dynamics of plant and mammal communities in South West Europe. Quaternary International 288, 63–72.

Malinverno, A., Ryan, W.B.F., 1986. Extension in the Tyrrenian Sea and shortening in the Apennines as result of arc migration driven by sinking of the lithosphere. Tectonics 5, 227–245.

Manzi, G., Magri, D., Milli, S., Palombo, M.R., Margari, V., Celiberti, V., Barbieri, M., Barbieri, M., Melis, R.T., Rubini, M., Ruffo, M., Saracino, B., Tzedakis, P.C., Zarattini, A., Biddittu, I., 2010. The new chronology of the Ceprano calvarium (Italy). Journal of Human Evolution 59, 580–585.

Marasti, R., 1991. Bivalvi polisiringi del Pliocene, viventi nel Mediterraneo: distribuzione e osservazioni paleoecologiche. 2° Parte. (Pliocene polysyringian Bivalves living in the mediterranean: distribution and paleoecological observations. Part 2). L'Ateneo Parmense. Acta Nat. 26, 39–63.

799 Mazza, P., Bertini, A., 2013. Were Pleistocene hippopotamuses exposed to climate-driven body size
800 changes? BOREAS 42, 194–209.
801 Meish, C., 2000. Freshwater Ostracoda of Western and Central Europe. In: Schwoerbel, J. and Zwick,
802 P., Eds., Süesswasserfauna von Mitteleuropa, 522 pp. Heidelberg, Berlin: Spektrum Akademischer
803 Verlag, no. 8/3.
804 Melis, R., Bernasconi, M.P., Colizza, E., Di Rita, F., Schneider, E.E., Forete, E., Montenegro, M.E.,
805 Pugliese, N., Ricci, M., 2015. Late Holocene palaeoenvironmental evolution of the northern
806 harbour at the Elaiussa Sebaste archaeological site (south-eastern Turkey): evidence from core
807 ELA6. Turkish Journal of Earth Sciences 24, 566–584.
808 Nara, M., 2002. Crowded *Rosselia socialis* in Pleistocene inner shelf deposits: benthic Paleoecology
809 during rapid sea-level rise. Palaios 17, 268–276.
810 Neale, J.V., 1988. Ostracods and paleosalinity reconstruction. In: De Deckker, P., Colin, J.-P.,
811 Peypouquet, J.-P. (Eds.), Ostracoda in the Earth Sciences. Elsevier, Amsterdam, pp. 125–155.
812 Nolf, D. 2013. The Diversity of Fish Otoliths Past and Present. Royal Belgian Institute of Natural
813 Sciences, Bruxelles, 350 pp.
814 Nordlie, F.C. 2003. Fish communities of estuarine salt marshes of Eastern North America, and
815 comparison with temperate estuaries of other continents. Reviews in Fish Biology and Fisheries
816 13, 281–325.
817 Orain, R., Lebreton, V., Ermolli, E.R., Combourieu-Nebout, N., Sémah, A.-M., 2013. *Carya* as marker
818 for tree refuges in southern Italy (Boiano basin) at the Middle Pleistocene. Palaeogeography,
819 Palaeoclimatology, Palaeoecology 369, 295–302.
820 Orain, R., Russo Ermolli, E., Lebreton, V., Di Donato, V., Bahain, J.-J., Sémah, A.-M., 2015.
821 Vegetation sensitivity to local environmental factors and global climate changes during the Middle
822 Pleistocene in southern Italy—A case study from the Molise Apennines. Review of Palaeobotany
823 and Palynology 220, 69–77.
824 Ori, G.G., Serafini, G., Visentin, C., Ricci Lucchi, F., Casnedi, R., Colalongo, M.L., Mosna, S., 1991.
825 The Plio-Pleistocene Adriatic foredeep (Marche and Abruzzo, Italy): an integrated approach to
826 surface and subsurface geology. Third Conference of European Association of Petroleum Geology,
827 Adriatic Foredeep Field Trip Guidebook, Florence, Italy. Milano, Agip S.p.A., pp. 85.

828 Pemberton, S.G., MacEachern, J.A., Dashtgard, S.E., Bann, K.L., Gingras, M.K., Zonneveld, J.-P.,
829 2012. Shorefaces. In: Knaust, D., and Bromley, R.G. (Eds.), Trace Fossils as Indicators of
830 Sedimentary Environments. Developments in Sedimentology, Elsevier, Amsterdam, 64, 563–603.
831 Paterson, A.W., Whitfield, A.K. 2000. The ichthyofauna associated with an intertidal creek and
832 adjacent eelgrass beds in the Kariega Estuary, South Africa. Environmental Biology of Fishes 58,
833 145–1565.
834 Peres J.M., Picard J., 1964. Nouveau manuel de bionomie bentique de la Mer Méditerranée. Rec. Trav.
835 St. Marine Endoume 31, 5–137.
836 Pizzi, A., 2003. Plio-Quaternary uplift rates in the outer zone of central Apennines fold-and-thrust belt,
837 Italy. Quaternary International 101–102, 299–237.
838 Platt, N.H., Wright, V.P., 1992. Palustrine carbonates at the Florida Everglades: towards an exposure
839 index for the freshwater environment. Journal of Sedimentary Petrology 62, 1058–1071.
840 Plint, A.G., McCarthy, P.J.M., Faccini, U.F., 2001. Nonmarine sequence stratigraphy: Updip
841 expression of sequence boundaries and systems tracts in a high-resolution framework, Cenomanian
842 Dunvegan Formation, Alberta foreland basin, Canada. American Association of Petroleum
843 Geologists Bulletin 85, 1967-2001.
844 Plint, A.G., Nummedal, D., 2000. The falling stage systems tract: recognition and importance in
845 sequence stratigraphy analysis. In: Hunt, D., Gawthorpe, R.L. (Eds.), Sedimentary Responses to
846 Forced Regression, Geol. Soc. London Spec. Publ. 172, 1–17.
847 Reuter, M., Piller, W.E., Harzhauser, M., Kroh, A., Berning, B., 2009. A fossil Everglades-type marl
848 prairie and its paleoenvironmental significance. Palaios 24, 747–755.
849 Ricci Lucchi, F., 1986. The Oligocene to Recent foreland basins in the northern Apennines. In: Allen,
850 P.A., Homewood, P. (Eds.), Foreland Basins, Int. Assoc. Sedimentol. Spec. Publ. 8, 105–139.
851 Rossi, V., Amorosi, A., Sarti, G., Potenza, M., 2011. Influence of inherited topography on the
852 Holocene sedimentary evolution of coastal systems: An example from Arno coastal plain
853 (Tuscany, Italy). Geomorphology 135, 117–128.
854 Russo Ermolli, E., 1994. Analyse pollinique de la succession lacustre pléistocène du Vallo di Diano
855 (Campanie, Italie). Annales de la Société géologique de Belgique 117, 333–354.

Russo Ermolli, E., Aucelli, P.P.C., Di Rollo, A., Mattei, M., Petrosino, P., Porreca, M., Rosskopf, C.M., 2010. An integrated stratigraphical approach to the Middle Pleistocene succession of the Sessano basin (Molise, Italy). Quaternary International 225, 114–127.

Russo Ermolli, E., Di Donato, V., Martín-Fernández, J.A., Orain, R., Lebreton, V., Piovesan, G., 2015. Vegetation patterns in the Southern Apennines (Italy) during MIS 13: Deciphering pollen variability along a NW-SE transect. Review of Palaeobotany and Palynology 218, 167–183.

Sadori, L., Giardini, M., Chiarini, E., Mattei, M., Papasodaro, F., Porreca, M., 2010. Pollen and macrofossil analyses of Pliocene lacustrine sediments (Salto river valley, Central Italy). Quaternary International 225, 44–57.

Sarti, G., Rossi, V., Amorosi, A., Bini, M., Giacomelli, S., Pappalardo, M., Ribecai, C., Ribolini, A., Sammartino, I., 2015. Climatic signature of two mid–late Holocene fluvial incisions formed under sea-level highstand conditions (Pisa coastal plain, NW Tuscany, Italy). Palaeogeography, Palaeoclimatology, Palaeoecology 424, 183–195.

Seike, K., Yanagishima, S., Nara, M., Sasaki, T., 2011. Large *Macaronichnus* in modern shoreface sediments: Identification of the producer, the mode of formation, and paleoenvironmental implications. Palaeogeography, Palaeoclimatology, Palaeoecology 311, 224–229.

Serandrei-Barbero, R., Albani, A., Donnici, S., Rizzetto, F., 2006. Past and recent sedimentation rates in the Lagoon of Venice (Northern Italy). Estuarine, Coastal and Shelf Science 69, 255–269.

Serandrei-Barbero, R., Bertoldi, R., Canali, G., Donnici, S., Lezziero, A., 2005. Paleoclimatic record of the past 22,000 years in Venice (Northearn Italy): Biostratigraphic evidence and chronology. Quaternary International 140–141, 37–52.

Stoops, G., 2003. Guidelines for Analysis and Description of Soil and Regolith Thin Sections. Soil Science Society of America, Madison WI, 184 pp.

Tzedakis, P.C., Hooghiemstra, H., Pälike, H., 2006. The last 1.35 million years at Tenaghi Philippon: revised chronostratigraphy and long-term vegetation trends. Quaternary Science Reviews 25, 3416–3430.

Vatova A., 1981. Recherches comparatives sur le “valli” salées de peche de la haute Adriatique. Rapp. Comm. Int. Mer. Médit. 27, 93–94.

884 Walker and Plint, 1992. Wave- and storm-dominated shallow marine systems., In: Walker R.G., James,
885 N.P. (Eds.), Facies models-response to sea-level changes: St. John's, Newfoundland, Canada,
886 Geological Association of Canada, p. 219–238.
887 Waren A., 1996. Ecology and systematics of the north European species of *Rissoa* and *Pusillina*
888 (Prosobranchia: Rissoidae). Journal of the Marine Biological Association, 76, 1013-1059.
889 Webb, C.J. 1980. Systematics of the *Pomatoschistus minutus* complex (Teleostei: Gobiidae).
890 Philosophical Transactions of the Royal Society 291, 201–241.
891 Zecchin, M., Brancolini, G., Tosi, L., Rizzetto, F., Caffau, M., Baradello, L., 2009. Anatomy of the
892 Holocene succession of the southern Venice lagoon revealed by very high-resolution seismic data.
893 Continental Shelf Research 29, 1343–1359.
894
895

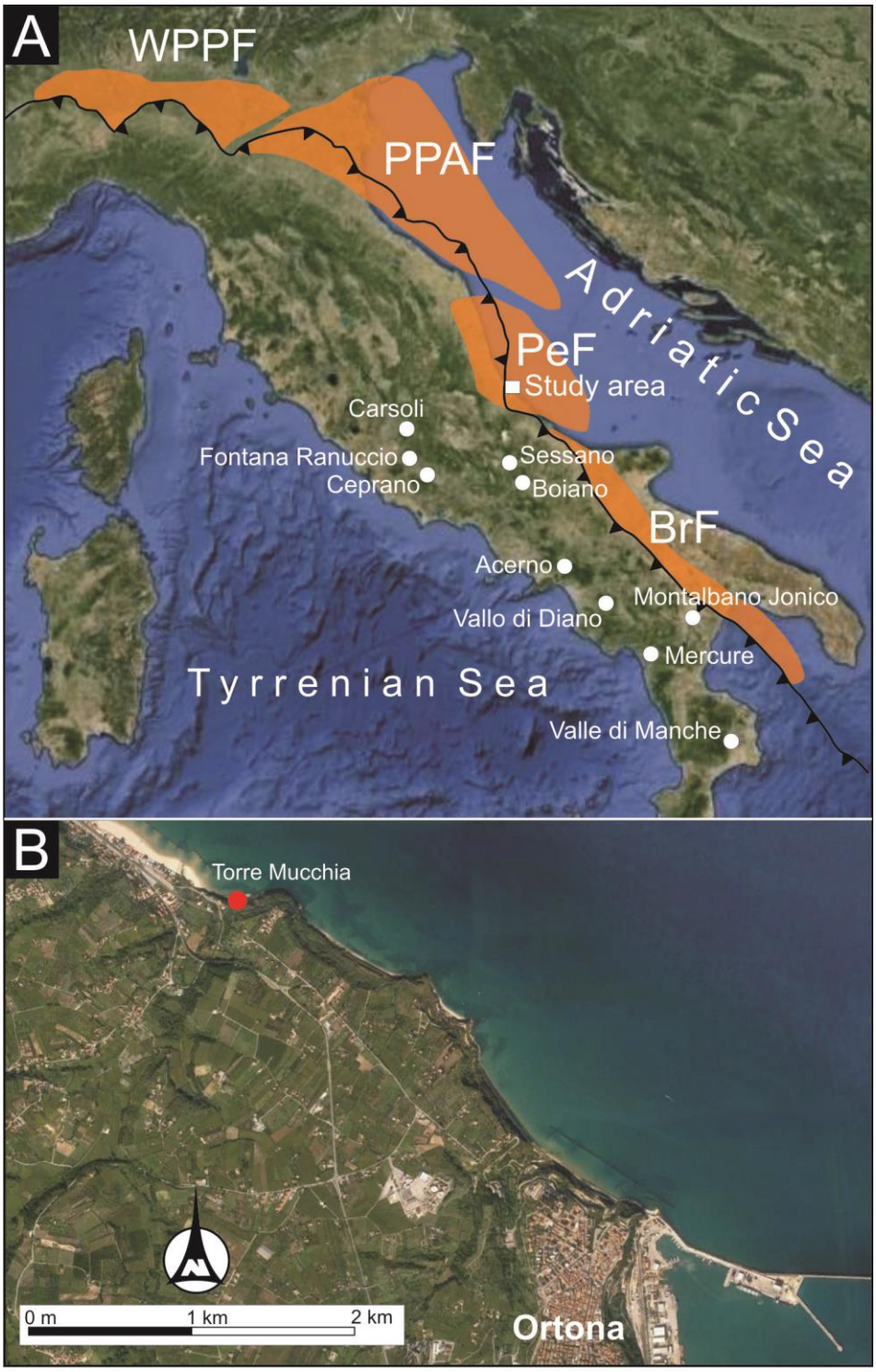
A
WPPF
PPAF
Adriatic Sea
PeF
Study area
Carsoli
Fontana Ranuccio
Ceprano
Sessano
Boiano
BrF
Acerno
Montalbano Jonico
Vallo di Diano
Mercure
Tyrrenian Sea
Valle di Manche
B
Torre Mucchia
0 m
1 km
2 km
Ortona

Figure 1

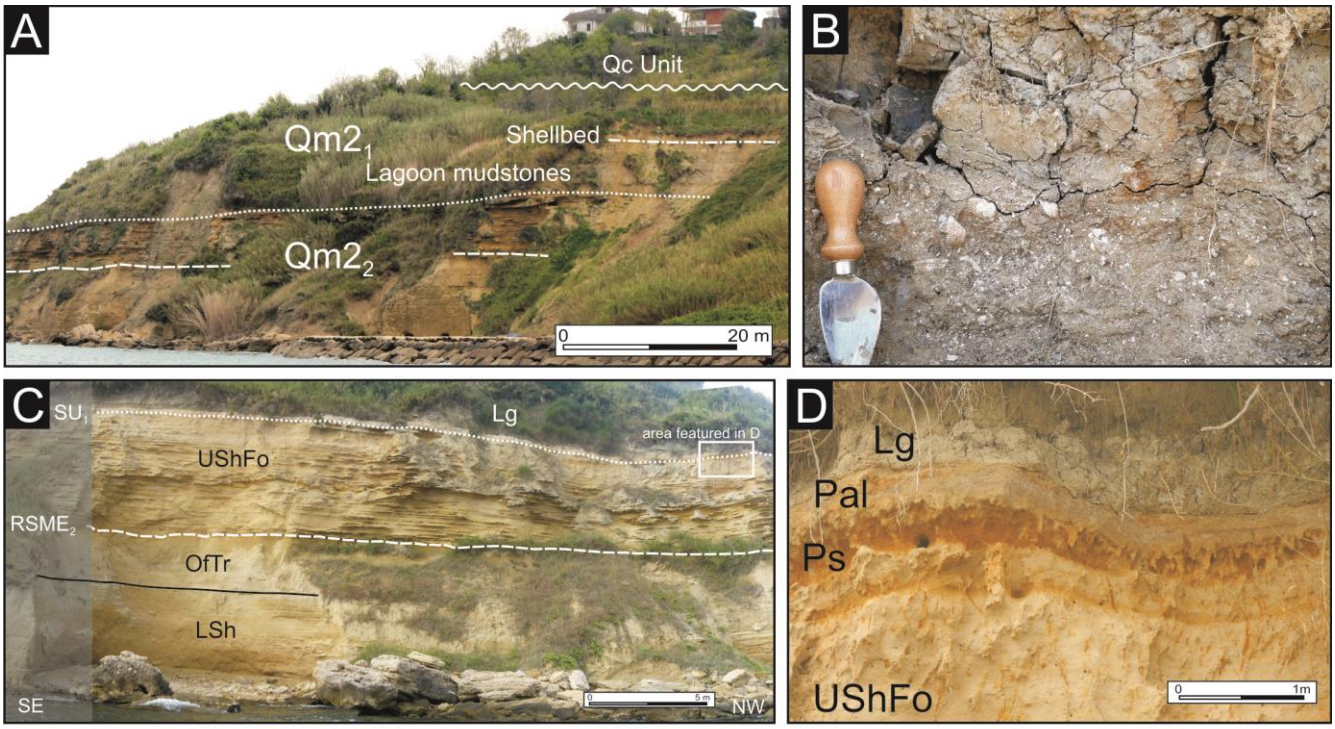
A
Qc Unit
Qm2$_1$
Shellbed
Lagoon mudstones
Qm2$_2$
0
20 m
B
C
SU$_1$
Lg
area featured in D
UShFo
RSME$_2$
OfTr
LSh
SE
NW
D
Lg
Pal
Ps
UShFo
0
1m

Figure 2

899

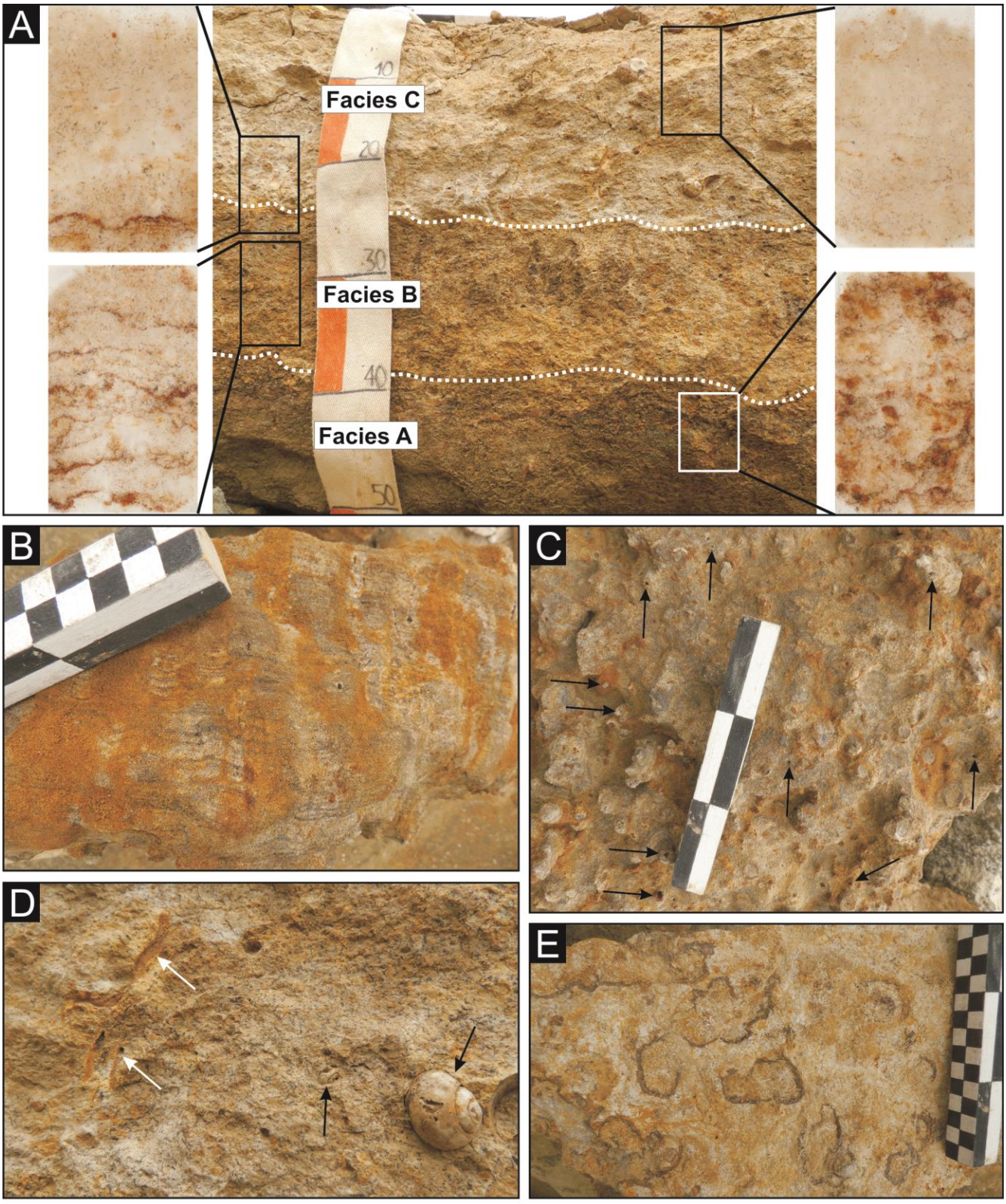

Figure 3

900

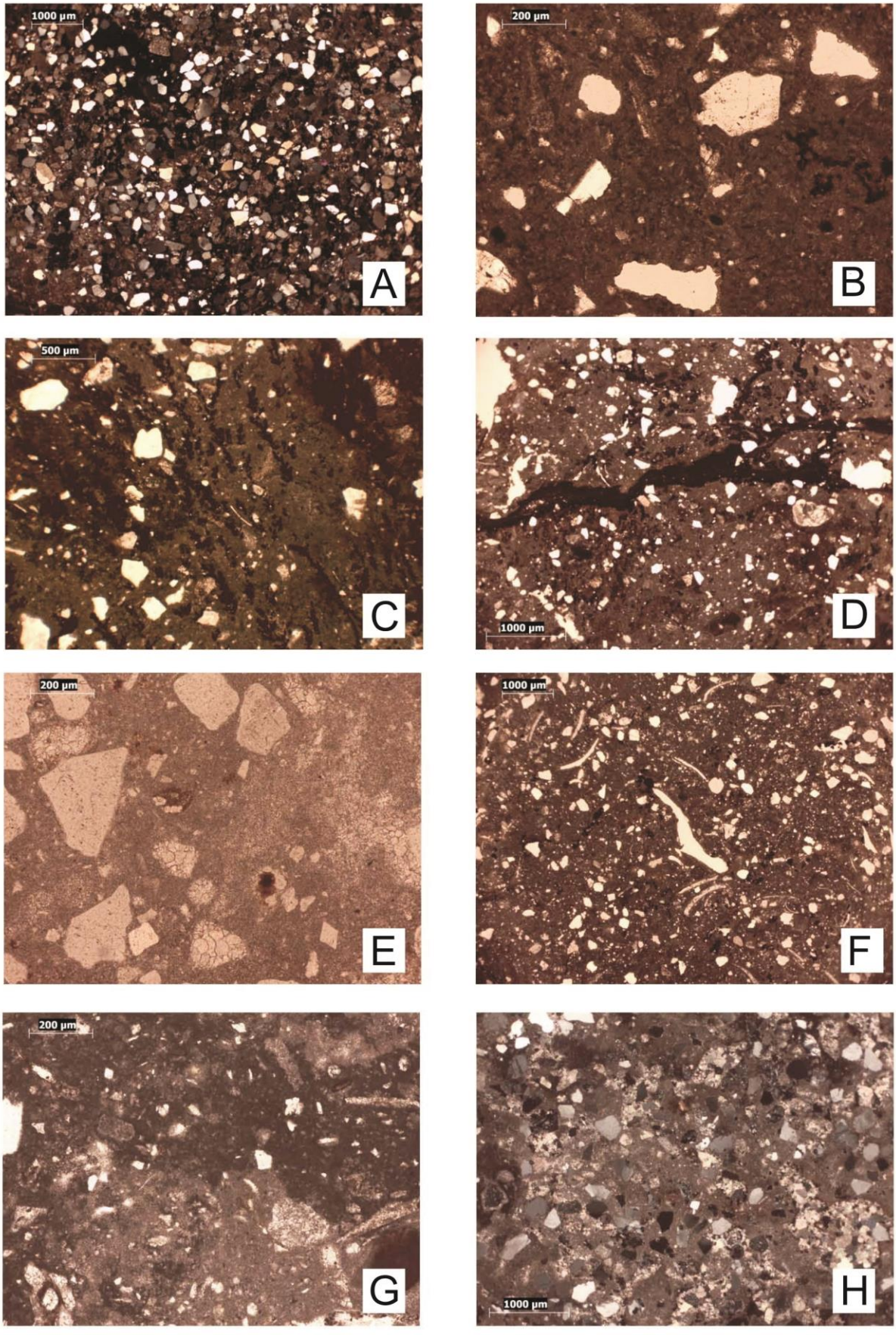
1000 µm
A
200 µm
B
500 µm
C
1000 µm
D
200 µm
E
1000 µm
F
200 µm
G
1000 µm
H

901

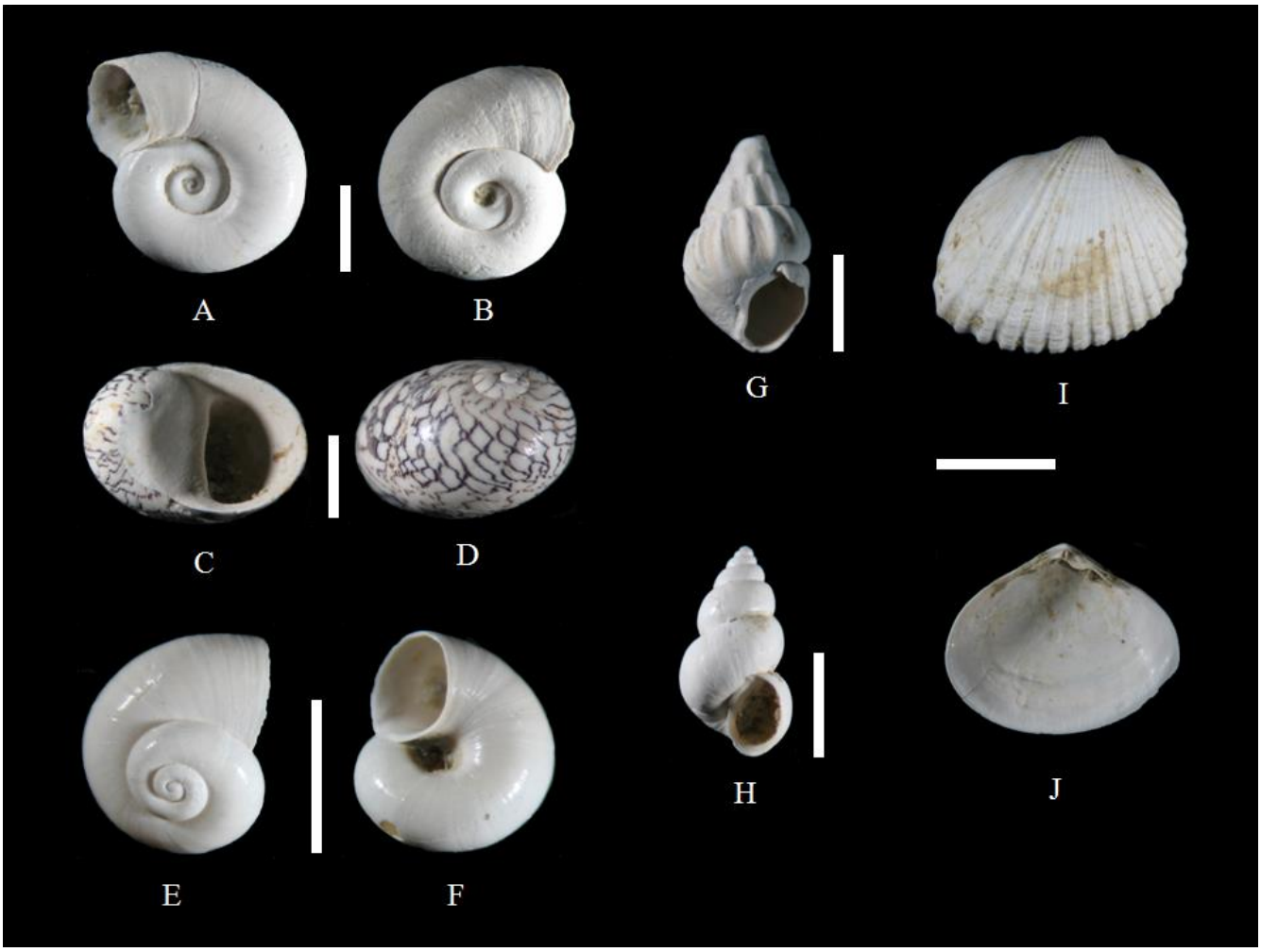

902

903

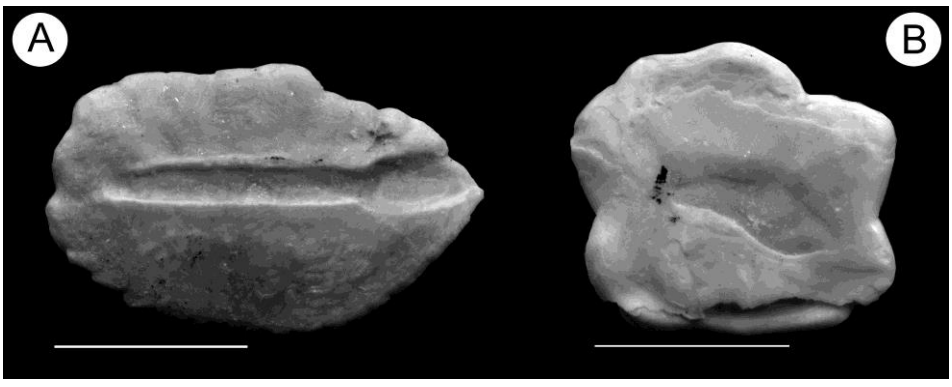

904

905

906

907

908

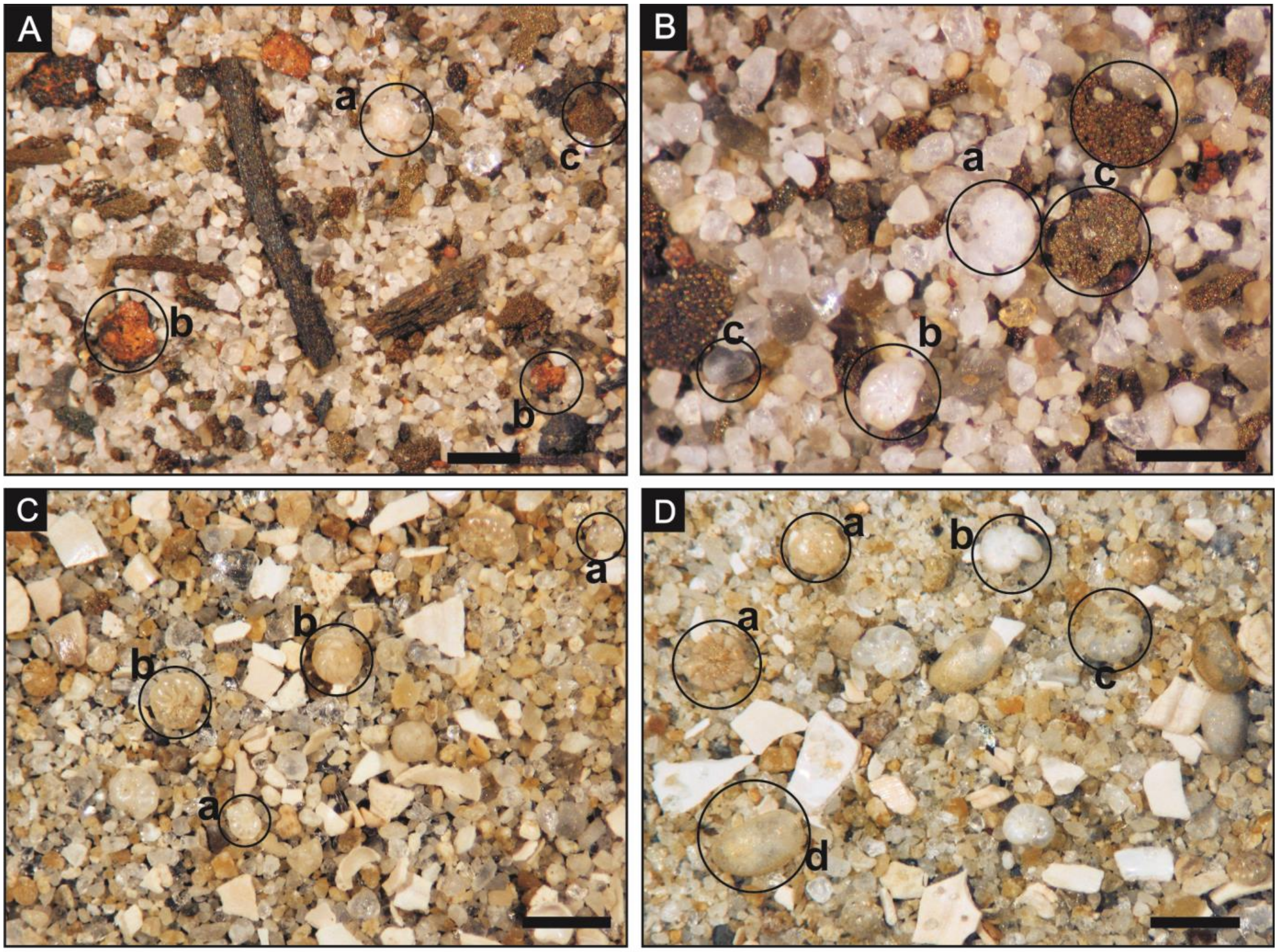
A
a
b
c
B
a
b
c
C
a
b
D
a
b
c
d

Figure 7

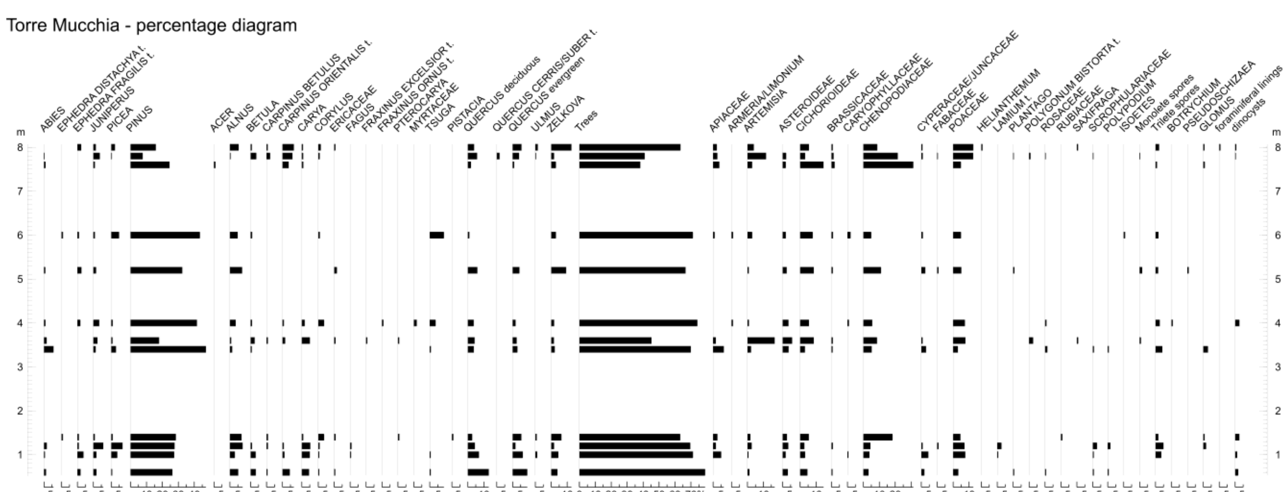
Torre Mucchia - percentage diagram
ABIES
EPHEDRA DISTACHYA t.
EPHEDRA FRAGILIS t.
JUNIPERUS
PICEA
PINUS
ACER
ALNUS
BETULA
CARPINUS BETULUS
CARPINUS ORIENTALIS t.
CARYA
CORYLUS
ERICACEAE
FAGUS
FRAXINUS EXCELSIOR t.
FRAXINUS ORNUS t.
PTEROCARYA
MYRTACEAE
TSUGA
PISTACIA
QUERCUS deciduous
QUERCUS CERRIS/SUBER t.
QUERCUS evergreen
ULMUS
ZELKOVA
Trees
APIACEAE
ARMERIA/LIMONIUM
ARTEMISIA
ASTEROIDEAE
CICHORIOIDEAE
BRASSICACEAE
CARYOPHYLLACEAE
CHENOPODIACEAE
CYPERACEAE/JUNCACEAE
FABACEAE
POACEAE
HELIANTHEMUM
LAMIUM t.
PLANTAGO
POLYGONUM BISTORTA t.
ROSACEAE
RUBIACEAE
SAXIFRAGA
SCROPHULARIACEAE
POLYPODIUM
ISOETES
Monolete spores
Trilete spores
BOTRYCHIUM
PSEUDOSCHIZAEA
GLOMUS
foraminiferal linings
dinocysts
m
8
7
6
5
4
3
2
1

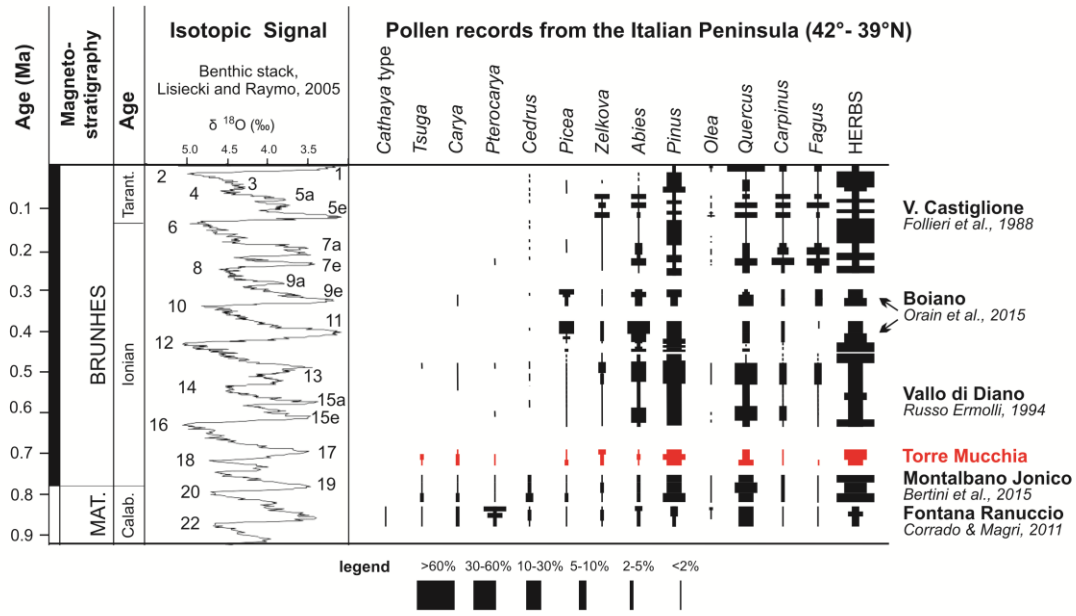
Age (Ma)
Magneto-stratigraphy
Age
Isotopic Signal
Benthic stack, Lisiecki and Raymo, 2005
δ 18O (‰)
5.0 4.5 4.0 3.5
Pollen records from the Italian Peninsula (42°- 39°N)
Cathaya type
Tsuga
Carya
Pterocarya
Cedrus
Picea
Zelkova
Abies
Pinus
Olea
Quercus
Carpinus
Fagus
HERBS
BRUNHES
MAT.
Tarant.
Ionian
Calab.
V. Castiglione
Follieri et al., 1988
Boiano
Orain et al., 2015
Vallo di Diano
Russo Ermolli, 1994
Torre Mucchia
Montalbano Jonico
Bertini et al., 2015
Fontana Ranuccio
Corrado & Magri, 2011
legend
>60% 30-60% 10-30% 5-10% 2-5% <2%

912

Supplementary Material

Sedimentology, faunal content and pollen record of Middle Pleistocene palustrine and lagoonal sediments from the Peri-Adriatic basin (Abruzzi, eastern central Italy)

Pierluigi Pieruccini, Claudio Di Celma, Federico Di Rita, Donatella Magri, Giorgio Carnevale, Piero Farabollini, Luca Ragaini, Mauro Caffau

Torre Mucchia pollen counts – Arboreal Pollen

Sample depth (m)	0.6	1	1.2	1.4	3.4	3.6	4	5.2	6	7.6	7.8	8
Abies	2	1	2	0	8	2	1	1		1	1	
Ephedra distachya t.				1					1			
Ephedra fragilis t.	3	6	1	1			3	2	3		1	
Juniperus	3	3	7	1	2	3	4	2	1	1	9	2
Picea	1	6	8	1	4	1	1		5		1	3
Pinus	40	43	31	31	63	21	45	38	44	25	17	20
Acer										1		
Alnus	8	5	9	8	2	1	4	9	5		1	7
Betula	5	5	1		1	3	1		1		8	1
Carpinus betulus	1		1	1		1					5	1
Carya	7	8	6	1		6	2			1	2	1
Corylus	1	1	1	4			4		1		2	2
Ericaceae	1			1		1		2				1
Fagus		1	1									
Fraxinus						1						
Fraxinus ornus t.							1					
Pterocarya				1		1						
Myrtaceae							2					
Carpinus orientalis t.	7	2	1			2	1			4	14	9
Tsuga	1	1			1		4		9			
Pistacia				1								
Quercus deciduous	20	11	5	3	5	5	4	7	1	2	13	5
Quercus cerris/suber											4	
Quercus evergreen	14	10	2	6	4	3	2	5		1	9	7
Ulmus		2		1							1	2
Zelkova	6	7	2	7	3	2	2	11	3	3	4	16

913